Precambrian Research 328 (2019) 217–234

Contents lists available at ScienceDirect

Precambrian Research

journal homepage: www.elsevier.com/locate/precamres

Ca. 1.04 Ga hot Grenville granites in the western Yangtze Block, southwest China

Yan-Jun Wang[a,b], Wei-Guang Zhu[a,*], Hui-Qing Huang[c], Hong Zhong[a], Zhong-Jie Bai[a], Hong-Peng Fan[a], Yi-Jin Yang[a]

[a] State Key Laboratory of Ore Deposit Geochemistry, Institute of Geochemistry, Chinese Academy of Sciences, 99 West Lincheng Road, Guiyang 550081, China
[b] University of Chinese Academy of Sciences, Beijing 100049, China
[c] Economic Geology Research Center, College of Science and Engineering, Division of Tropical Environments and Societies, James Cook University, Townsville, QLD 4811, Australia

ARTICLE INFO

Keywords:
A-type granites
Hot granite
Yangtze Block
Grenville orogeny

ABSTRACT

The late Mesoproterozoic to early Neoproterozoic magmatism in the western Yangtze Block, though minor in volume, has offered a rare opportunity for understanding the role of the Yangtze Block in the Grenville orogeny. The Huidong K-feldspar granites have SIMS zircon U-Pb ages of 1048.5 ± 4.9 Ma and 1043.1 ± 5.1 Ma, whereas the Yuanmou biotite granites were dated at 1041 ± 12 Ma by LA-ICP-MS. Their ages are indistinguishable within error, suggesting that they were emplaced contemporaneously. Both Huidong and Yuanmou rocks show geochemical features typical of A-type granites, including high FeO^*/MgO, Ga/Al ratios and elevated contents of high-field-strength elements (HFSE). The Huidong granites exhibit positive whole-rock $\varepsilon_{Nd}(t)$ (+0.58 to +4.4) and zircon $\varepsilon_{Hf}(t)$ (+6.0 to +8.3) values close to those of regional coeval mafic rocks. They have a narrow range of zircon $\delta^{18}O$ from 6.2‰ to 7.2‰, which is only slightly higher than the 'mantle zircon' value of 5.3 ± 0.6‰. High Nb/La and Nb/Th ratios in these rocks overlap with those of regional coeval mantle-derived rocks. Along with high zircon saturation temperatures of > 1000 °C, we suggest that the Huidong granites could have formed mainly by extreme fractionation from basaltic parental magmas, or alternatively by partial melting of newly emplaced tholeiite at high temperatures. By contrast, the Yuanmou granites have lower whole-rock $\varepsilon_{Nd}(t)$ (−2.0 to +0.59) and zircon $\varepsilon_{Hf}(t)$ (−1.5 to +5.1) values and a Hf isotope crustal model age of ~1.56–1.97 Ga, suggesting that its parental magmas may be generated by partial melting of old crust during intrusion of mantle-derived magmas. Ca. 1.04 Ga granites in the region show geochemical features similar to A-type granites in orogenic belts, e.g., the aluminous A-type granites in the Lachlan Fold Belt, Southeast Australia. They are also characterized by high-extremely high (> 1000 °C) temperature in their genesis, similar to coeval hot Grenville granites globally. Temporal correlation of metamorphic and magmatic records between South China and the Grenville Province leads us to conclude that the ~1.04 Ga A-type granites in the western Yangtze Block form parts of the hot Grenville granites emplaced during post-orogenic crustal extension.

1. Introduction

Grenville orogeny (ca. 1.3–0.9 Ga) represents collisional events in the assembly of the Neoproterozoic Rodinia supercontinent (e.g., Li et al., 2008). In South China, the Sibao (or Jiangnan) orogen is widely believed to have recorded the amalgamation between Yangtze and Cathaysia blocks, although precise timing and evolution of the orogen remain highly controversial (e.g., Li et al., 2002; Wang et al., 2007; Chen et al., 2018). The Sibao orogen has been proposed to form part of the Grenville orogen based on multiple lines of evidence (e.g., Li et al., 2002, 2007, 2008; Greentree et al., 2006; Ye et al., 2007; Zhang et al., 2007; Yang et al., 2009; Yao et al., 2017). In this model, South China fits in the center of the Rodinia supercontinent and represents a link between Australia-east Antarctica and Laurentia (Li et al., 1995). However, some researchers consider that the Sibao orogen may be younger than the Grenville orogen. They suggest that convergence between the Yangtze and Cathaysia blocks started in the earliest Neoproterozoic and continued to ~800 Ma (Wang et al., 2007, 2013; Zhao et al., 2011). These researchers also believe that South China was not in the center in the configuration of Rodinia, but in the periphery of the supercontinent (Zhao et al., 2011).

Recently, some 1.16–1.02 Ga magmatic rocks have been discovered

* Corresponding author.
E-mail address: zhuweiguang@vip.gyig.ac.cn (W.-G. Zhu).

https://doi.org/10.1016/j.precamres.2019.04.024
Received 13 November 2018; Received in revised form 20 March 2019; Accepted 21 April 2019
Available online 22 April 2019
0301-9268/

in the western Yangtze Block (Greentree et al., 2006; Chen et al., 2014, 2018; Zhu et al., 2016; Geng et al., 2017), as well as in the eastern Yangtze Block (Li et al., 2013a; Wang et al., 2018). These rocks provide a window to gain insight into the tectonic evolution of the Yangtze Block in the late Mesoproterozoic time and to test the two contrasting models outlined above. Published results show that the 1.16–1.02 Ga magmatism has produced alkaline basalts, tholeiitic basalts and some A-type granitic rocks, likely in an extensional setting associated with continental rifting (Greentree et al., 2006; Zhu et al., 2016; Chen et al., 2018), but the geodynamic process that led to the continental extension remains debated. Chen et al. (2014, 2018) and Wang et al. (2018) suggested that intrusion of these rocks is inconsistent with Yangtze bearing part of the Grenville orogen. However, similar magmatic suites have been found in orogenic belts globally, e.g., the Paleozoic Lachlan Fold Belt in southeast Australia (Collins, 2002). In this paper, we present new data for some newly recognized late Mesoproterozoic granitic rocks and revisit the genesis of the ~1.04 Ga rock suites in the western Yangtze Block. We also compare the metamorphic and magmatic records in South China with those in Grenville orogen and find a close match between them.

2. Geological background and petrography

The South China Craton consists of the Yangtze Block in the northwest and the Cathaysia Block in the southeast, bounded by the Sibao orogen between them (Fig. 1a; Li et al., 2007). The oldest rocks ever reported for the Yangtze Block are the Archean Kongling tonalitic-trondhjemitic-granodioritic (TTG) gneisses complex (Qiu et al., 2000; Gao et al., 2011). It has been suggested that Archean materials may be widespread in this block on the basis of U-Pb and Lu-Hf isotopic data from inherited zircons in magmatic rocks and detrital zircons from sedimentary rocks (Zhang et al., 2006; Zheng et al., 2006; Zhao et al., 2010; Wang et al., 2012a). Late Paleoproterozoic to early Mesoproterozoic meta-volcanic and sedimentary sequences crop out from north to south in the western Yangtze Block, including the Dahongshan, Hekou, Dongchuan (Lower Kunyang) Groups and Tongan Formation (Lower Huili Group). Tufaceous and volcanic layers in these strata, together with mafic intrusions and detrital zircons, well constrain the depositional ages of these groups at ~1.75–1.50 Ga (Greentree and Li, 2008; Zhao et al., 2010; Geng et al., 2012, 2017; Chen et al., 2013; Fan et al., 2013).

Late Mesoproterozoic to early Neoproterozoic rocks, such as the Upper Kunyang, Upper Huili and Julin Groups, are also widespread in the western Yangtze Block. Tuff samples from the Heishantou Formation of the Upper Kunyang Group contain abundant zircons, which were determined to yield SHRIMP U-Pb ages of 995 ± 15 Ma and 1032 ± 9 Ma (Greentree et al., 2006; Zhang et al., 2007). Meanwhile, U-Pb data of detrital zircons from the Upper Kunyang Group suggest a youngest depositional age at ~960 Ma (Greentree et al., 2006). The Upper Huili Group contains the Limahe, Fengshanying and Tianbaoshan Formations from base upwards. The Limahe and Fengshanying Formations comprise meta-sedimentary rocks, including sandstone, slate, schist, quartzite and dolomite. The lower part of Tianbaoshan Formation is also dominated by meta-sedimentary rocks, whereas the upper part of Tianbaoshan Formation comprises dacitic-rhyolitic lavas and tufaceous rocks, with minor schist, meta-sandstone and carbonate layers. The Tianbaoshan volcanic rocks were dated at 1021 ± 6.4 Ma, 1025 ± 13 Ma and 1028 ± 9 Ma by SIMS zircon U-Pb methods (Geng et al., 2007; Zhu et al., 2016). Spatially-associated mafic dykes also yield SIMS zircon U-Pb age of 1023 ± 6.7 Ma (Zhu et al., 2016).

The Julin Group, with a total thickness of > 3560 m, is composed of the Pudeng, Lugumo, Fenghuangshan and Haizishao Formations from the bottom to top. The group consists mainly of slate, gneiss, schist, sandstone, marble and dolomite with subordinate meta-volcanic rocks. Meta-basalts from the Julin Group have LA-ICP-MS zircon U-Pb ages of 1043 ± 19 Ma and 1050 ± 14 Ma (Chen et al., 2014). These geochronological data indicate that the Julin Group is an analogue to the Upper Kunyang and Huili Groups.

In this study, late Mesoproterozoic Huidong and Yuanmou granite samples were collected from the Huidong and Yuanmou counties, respectively (Fig. 1b–d). The Huidong granites have experienced little deformation and metamorphism. Field investigations show that the Huidong granites intrude the Upper Huili Group and have developed along a north-south fault system in several plutons (Fig. 1c), with a total outcrop area of around 2.5 km^2. The Huidong samples are mostly pink in color and coarse- to medium-grained (Fig. 2a). They are dominated by K-feldspar (~40–50%) and quartz (~35–40%), with minor plagioclase (~5–10%), Fe-Ti oxides (~3–5%), accessory minerals of zircon, chlorite, and allanite (Fig. 2b). K-feldspar grains are generally ~1 cm in length. Feldspars are commonly subjected to argillic alteration. The Yuanmou granites were emplaced into the Julin Group. Samples are mostly pale grey in color and medium-grained (Fig. 2c) and are composed of quartz (~35–45%), plagioclase (~30–35%), biotite (~5–10%), muscovite (~1–3%), accessory minerals of Fe-Ti oxides (~1–3%), chlorite and zircon (Fig. 2d). Muscovite is secondary; argillic alteration of feldspars occurs pervasively.

3. Analytical methods

Zircon grains (samples CYZ1304, CYZ1311, and 14YM02-03) were separated using conventional heavy liquid and magnetic techniques and further handpicked under binocular microscopes. They were subsequently mounted in epoxy resin, polished, and coated with gold film. Cathodoluminescence (CL) images and transmitted and reflected light microphotographs were taken to reveal internal structures of zircon grains. The U-Pb isotopic analyses of samples CYZ1304 and CYZ1311 were conducted using a Cameca IMS-1280 SIMS at the Ion Microprobe Laboratory of the Institute of Geology and Geophysics, Chinese Academy of Sciences (IGGCAS) in Beijing. Detailed analytical procedure was similar to that reported in Li et al. (2009b). The ellipsoidal spot is about 20 × 30 μm in size. Analyses of zircon standard 91,500 was interspersed with unknowns. The measured compositions are presented after correcting for common Pb using non-radiogenic ^{204}Pb. The uncertainties in ages are cited as 1σ, and the weighted mean ages are quoted at the 95% confidence level (2σ). Qinghu zircons were analyzed for quality check and yield a U-Pb age of 163.4 ± 5.6 Ma, indistinguishable from the recommended value (Li et al., 2013b). On the other hand, the U-Pb isotopes of sample 14YM02-03 were analyzed using an Agilent 7700x ICP-MS coupled with a NWR UP-213 laser ablation system at the University of Newcastle, Australia. A spot size of 40 μm and an ablation rate of 5 Hz were used. Detailed method was similar to that described in Offler and Huang (2018). Downhole fractionation and instrumental drift correction were completed using Iolite 2.5 (Paton et al., 2010).

Zircon oxygen isotopic analyses were also conducted on the Cameca IMS-1280 SIMS. A ~20 μm beam was adopted for analysis. Each analysis includes the pre-sputtering for 2 min, automatic beam centering for ~60 s, and integration of oxygen isotopes for 20 cycles × 4 s. Uncertainty for each analysis is generally better than 0.3–0.4‰ (1σ). The Penglai and Qinghu zircon standards were analyzed for calibration and quality check, respectively. The obtained $^{18}O/^{16}O$ values were presented after normalization to Vienna Standard Mean Ocean Water compositions (VSMOW, $^{18}O/^{16}O = 0.0020052$) and correction for the IMF. Measurements of the Qinghu zircon grains have an arithmetic mean of $\delta^{18}O = 5.50 \pm 0.21‰$, identical to the documented value of 5.4 ± 0.2‰ (Li et al., 2013b).

Analyses of zircon Lu-Hf isotopes were performed on a Neptune Plus multiple collector inductively coupled plasma mass spectrometer (MC-ICP-MS) with a GeoLas 2005 laser system at the State Key Laboratory of Geological Processes and Mineral Resources, China University of Geosciences (Wuhan). Detailed operating conditions and data

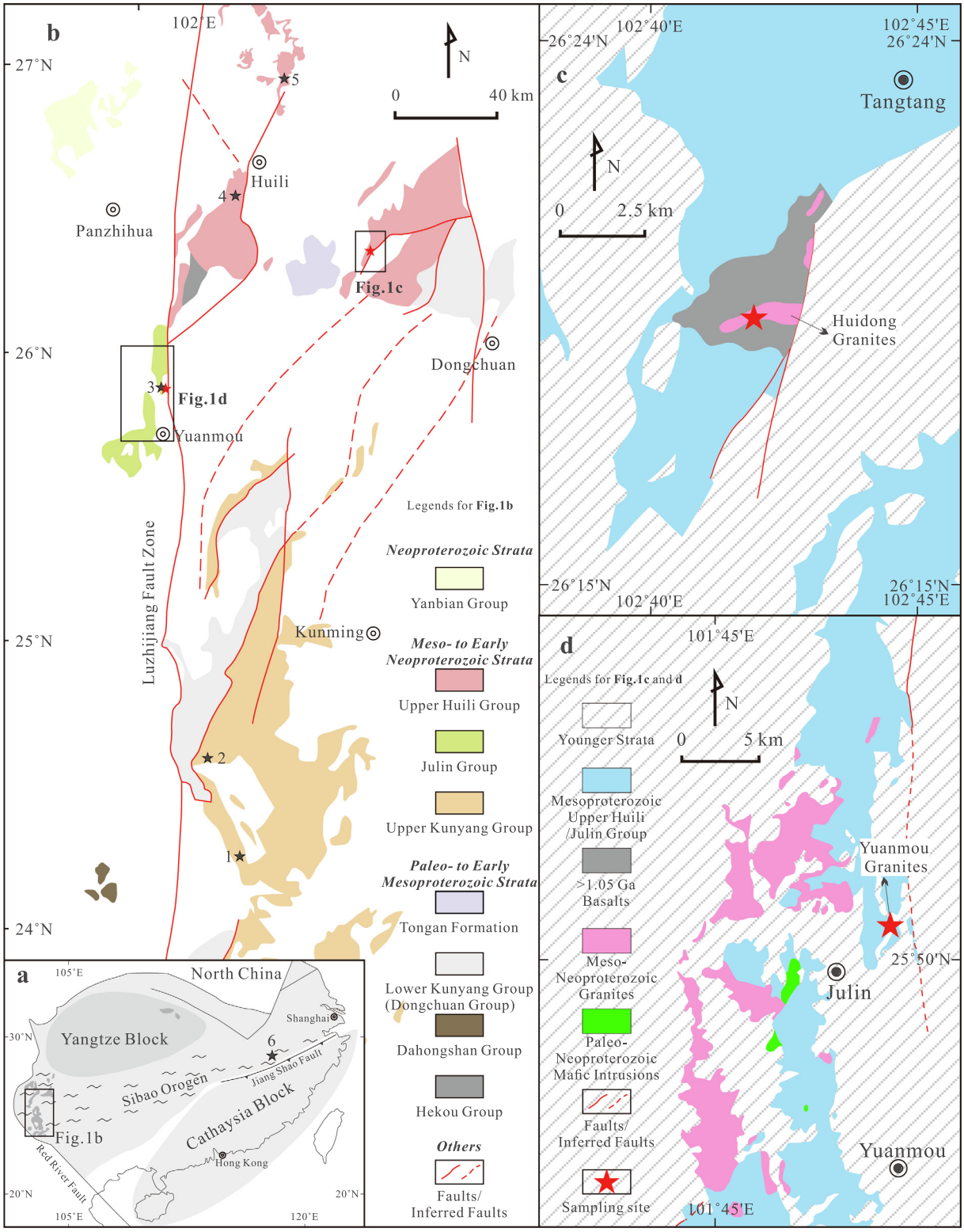

Fig. 1. (a) A simplified tectonic map showing the locations of the study area in the South China (Li et al., 2007) and (b) geological map showing the distribution of Proterozoic strata in the Kangdian region, SW, China (modified from Zhu et al. (2016)). Simplified geological maps for (c) the Huidong granites in the Tangtang town of Huidong County, Sichuan Province (modified from the Huili 1:200,000 geological map by SBG (1967)), and (d) the Yuanmou granites in the Yuanmou County, Yunnan Province (modified from Chen et al. (2018)). Numbers 1–6 with black stars represent the reported late Mesoproterozoic geochronological data: *1,* 995 ± 15 Ma and 1032 ± 9 Ma tuff and ignimbrite (Greentree et al., 2006; Zhang et al., 2007); *2,* 1142 ± 16 Ma alkali basalts (Greentree et al., 2006); *3,* 1050 ± 14 Ma meta-basalts and coeval felsic intrusions (Chen et al., 2014, 2018); *4–5,* 1025 ± 13 Ma and 1021 ± 6.4 Ma felsic volcanic rocks with coeval 1023 ± 6.7 Ma mafic dykes (Zhu et al., 2016); *6,* 1159 ± 8 Ma A-type rhyolites (Li et al., 2013a,b) and 1012 ± 4 Ma to 980 ± 5 Ma OIB-like basalts (Wang et al., 2018).

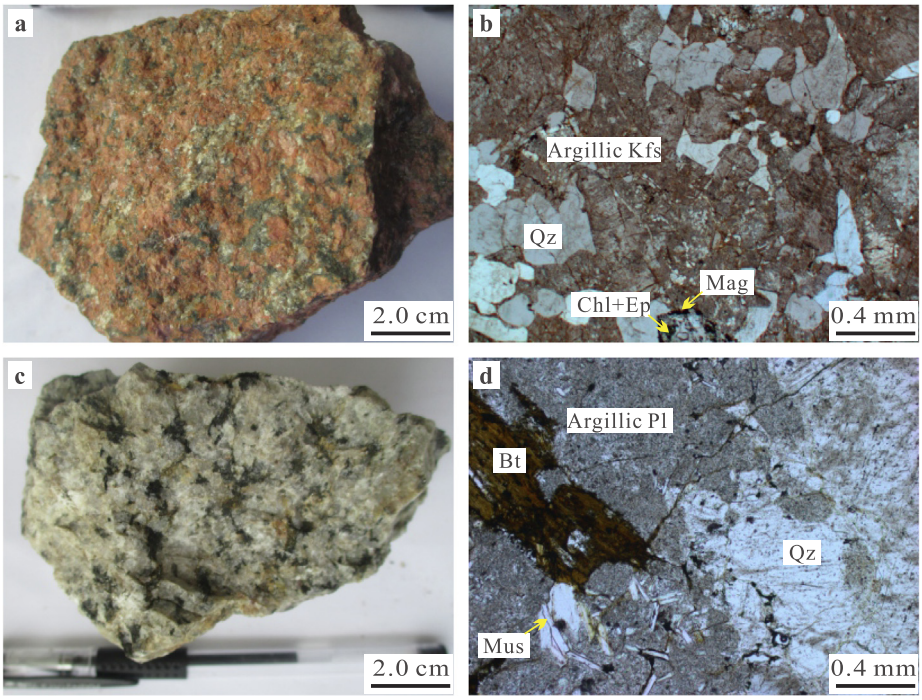

Fig. 2. Photos and photomicrographs showing petrographical and textural characteristics of the Huidong (a, b) and Yuanmou (c, d) granites. Abbreviations are Bt for biotite, Chl for chlorite, Ep for epidote, Kfs for potassium feldspar, Mag for magnetite, Mus for muscovite, Pl for plagioclase, and Qz for quartz.

acquisition method were similar to those described by Hu et al. (2012). The isobaric interference of ^{176}Lu on ^{176}Hf was corrected by measuring the intensity of the interference-free ^{175}Lu isotope and using the recommended $^{176}Lu/^{175}Lu$ ratio of 0.02656 (Blichert-Toft and Albarede, 1997) to calculate $^{176}Lu/^{177}Hf$ ratios. The interference of ^{176}Yb on ^{176}Hf was corrected by measuring the interference-free ^{173}Yb isotope and using the recommended $^{176}Yb/^{173}Yb$ ratio of 0.79639 (Fisher et al., 2014) to calculate $^{176}Hf/^{177}Hf$ ratios. Offline data reduction of signal selection, integration of selected signals and mass bias calibrations, was carried out using the ICPMSDataCal software (Liu et al., 2010). Zircon standard 91,500 was used for time-drift correction and external calibration. The calculations of the initial $^{176}Hf/^{177}Hf$ ratios were based on the measured $^{176}Hf/^{177}Hf$ ratios and a ^{176}Lu decay constant of $1.867 \times 10^{-11}\ a^{-1}$ (Söderlund et al., 2004). The calculations of ε_{Hf} values were according to chondritic ratios of $^{176}Hf/^{177}Hf = 0.282772$ and $^{176}Lu/^{177}Hf = 0.0332$ (Blichert-Toft and Albarede, 1997). Single-stage model ages (T_{DM1}^{Hf}) were calculated using the present-day $^{176}Hf/^{177}Hf$ ratio of 0.28325 and $^{176}Lu/^{177}Hf$ ratio of 0.0384 (Griffin et al., 2002). Two-stage model ages (T_{DM2}^{Hf}) were calculated by projecting the initial $^{176}Hf/^{177}Hf$ ratios back to the depleted mantle model growth curve with assuming a mean $^{176}Lu/^{177}Hf$ ratio of 0.015 for the average continental crust (Griffin et al., 2002).

Major element compositions were determined using X-ray fluorescence spectrometers (XRF) at ALS Chemex Co Ltd, Guangzhou. The analytical precision is estimated to be better than 5%. Trace elements were analyzed on a Perkin-Elmer Sciex ELAN DRC-e ICP-MS at the State Key Laboratory of Ore Deposit Geochemistry (SKLOG), Institute of Geochemistry of Chinese Academy of Sciences (IGCAS). Fifty milligrams of powered samples were dissolved with HF + HNO_3 mixture in high-pressure Teflon bombs at ~190 °C for 48 h as the procedures described by Qi et al. (2000). Rh was applied as an internal standard to monitor signal drift during counting. The international standards GBPG-1, OU-6, and the Chinese National standards GSR-1 and GSR-3, were used for analytical quality control. Analytical precision is typically better than 10%.

Samples for Nd isotopic analysis were spiked and dissolved in Teflon bombs with HF + HNO_3 + $HClO_4$ mixture, and subsequently separated using conventional cation-exchange techniques. The isotopic determination was conducted on a Finnigan MAT 262 multi-collector mass spectrometer at the Laboratory for Radiogenic Isotope Geochemistry, Institute of Geology and Geophysics (Beijing), Chinese Academy of Sciences. The obtained $^{143}Nd/^{144}Nd$ ratios were normalized to $^{143}Nd/^{144}Nd = 0.7219$ to correct for mass fractionation.

4. Analytical results

4.1. Zircon U-Pb dating

4.1.1. Age of the Huidong granites

Geochronological data for the Huidong and Yuanmou granites are listed in Tables 1 and 2. Two Huidong granite samples, CYZ1304 and CYZ1311, were selected for dating. Zircon grains of CYZ1304 are mostly euhedral, 80–180 μm in length, and with length to width ratios varying from 1:1 to 3:2. They display weak oscillatory zoning in CL images. Eighteen spot analyses on 18 zircons reveal that these grains have identical uranium (109–205 ppm), thorium (76–223 ppm) contents and Th/U ratios (0.71–0.99). All of the 18 analyses give concordant U-Pb ages, and generate a cluster with a weighted average $^{206}Pb/^{238}U$ age of 1048.5 ± 4.9 Ma (2σ, MSWD = 1.2) (Fig. 3a). This age is interpreted to represent the crystallization age for sample CYZ1304.

Zircons of sample CYZ1311 are similar to those of sample CYZ1304 in size and structure as revealed by CL images. Eighteen analyses of 18 zircons conducted on Cameca SIMS have a narrow range of U (94–244 ppm), Th (53–260 ppm) and U/Th ratios (0.48–1.07). All of the 18 measurements form a cluster in concordant curve with a weighted mean $^{206}Pb/^{238}U$ age of 1043.1 ± 5.1 Ma (2σ, MSWD = 0.71) (Fig. 3b), indistinguishable from that of sample CYZ1304 within analytical error.

4.1.2. Age of the Yuanmou granites

Sample 14YM02-03 is collected from Yuanmou. Prismatic zircons of sample 14YM02-03 are 80–150 μm in length, with length to width ratios of 3:2–2:1 and exhibiting clear oscillatory zoning in CL images.

Table 1
Cameca SIMS zircon U-Pb isotopic analyses for the Huidong granites in the western Yangtze Block.

Spot	U (ppm)	Th (ppm)	Th/U	$^{206}Pb/^{204}Pb_{measured}$	f_{206} (%)	Isotopic ratio						Age/Ma					
						$^{207}Pb^*/^{206}Pb^*$	± 1σ (%)	$^{207}Pb^*/^{235}U$	± 1σ (%)	$^{206}Pb^*/^{238}U$	± 1σ (%)	$^{207}Pb/^{206}Pb$	± 1σ	$^{207}Pb/^{235}U$	± 1σ	$^{206}Pb/^{238}U$	± 1σ
CYZ1304 (A granitic sample from Huidong area: N 26°19′18.1″, E 102°41′30.8″)																	
1	139	101	0.72	39,311	0.05	0.0740	0.57	1.8275	1.61	0.1791	1.50	1041	11	1055	11	1062	15
2	114	83	0.73	89,473	0.02	0.0746	0.60	1.8174	1.62	0.1768	1.50	1057	12	1052	11	1049	15
3	131	95	0.72	12,165	0.15	0.0731	0.70	1.7854	1.66	0.1771	1.51	1017	14	1040	11	1051	15
4	208	178	0.86	44,504	0.04	0.0742	0.46	1.8345	1.58	0.1794	1.51	1046	9	1058	10	1064	15
5	109	76.2	0.70	27,819	0.07	0.0744	0.69	1.7993	1.67	0.1753	1.52	1053	14	1045	11	1041	15
6	134	97.4	0.73	57,409	0.03	0.0735	0.63	1.8050	1.64	0.1782	1.51	1027	13	1047	11	1057	15
7	156	123	0.78	21,192	0.09	0.0737	0.64	1.8119	1.64	0.1783	1.51	1034	13	1050	11	1058	15
8	225	223	0.99	32,554	0.06	0.0740	0.45	1.8125	1.58	0.1776	1.52	1042	9	1050	10	1054	15
9	130	96.8	0.75	22,569	0.08	0.0740	0.61	1.8306	1.64	0.1794	1.52	1042	12	1057	11	1064	15
10	119	87.1	0.73	33,896	0.06	0.0741	0.62	1.8488	1.66	0.1809	1.54	1045	12	1063	11	1072	15
11	207	172	0.83	45,179	0.04	0.0736	0.49	1.7969	1.58	0.1771	1.50	1031	10	1044	10	1051	15
12	154	92.5	0.60	27,875	0.07	0.0747	0.67	1.8033	1.67	0.1751	1.52	1060	13	1047	11	1040	15
13	145	110	0.76	70,375	0.03	0.0743	0.56	1.8177	1.60	0.1773	1.50	1051	11	1052	11	1052	15
14	137	105	0.77	83,782	0.02	0.0745	0.55	1.8042	1.63	0.1757	1.53	1054	11	1047	11	1044	15
15	206	170	0.83	9913	0.19	0.0738	0.53	1.7683	1.64	0.1737	1.55	1037	11	1034	11	1032	15
16	119	84.1	0.71	37,027	0.05	0.0750	0.60	1.8187	1.62	0.1760	1.50	1068	12	1052	11	1045	15
17	190	176	0.93	164,091	0.01	0.0751	0.53	1.8149	1.62	0.1753	1.53	1071	11	1051	11	1041	15
18	210	202	0.96	43,403	0.04	0.0741	0.53	1.8101	1.60	0.1772	1.51	1044	11	1049	11	1052	15
CYZ1311 (A granitic sample from Huidong area: N 26°19′00.0″, E 102°41′14.4″)																	
1	187	145	0.77	31,458	0.06	0.0744	0.59	1.7847	1.63	0.1740	1.52	1052	12	1040	11	1034	14
2	171	123	0.72	54,046	0.03	0.0741	0.49	1.8109	1.59	0.1773	1.51	1043	10	1049	10	1052	15
3	138	109	0.79	24,850	0.08	0.0743	0.59	1.7815	1.62	0.1738	1.50	1051	12	1039	11	1033	14
4	180	94.6	0.53	32,663	0.06	0.0745	0.51	1.8055	1.59	0.1757	1.51	1056	10	1047	10	1043	15
5	94.2	53.1	0.56	19,239	0.10	0.0737	0.98	1.7587	1.82	0.1731	1.53	1033	20	1030	12	1029	15
6	114	54.9	0.48	19,886	0.09	0.0737	0.67	1.8022	1.65	0.1773	1.51	1034	14	1046	11	1052	15
7	117	72.3	0.62	24,942	0.07	0.0740	0.63	1.8185	1.63	0.1781	1.50	1043	13	1052	11	1057	15
8	164	142	0.87	13,031	0.14	0.0736	0.68	1.7664	1.65	0.1741	1.51	1031	14	1033	11	1034	14
9	102	65.3	0.64	13,075	0.14	0.0733	0.83	1.7855	1.72	0.1767	1.51	1022	17	1040	11	1049	15
10	244	260	1.07	79,419	0.02	0.0748	0.60	1.8042	1.62	0.1749	1.50	1063	12	1047	11	1039	14
11	122	88.9	0.73	20,943	0.09	0.0744	0.63	1.7922	1.68	0.1747	1.55	1052	13	1043	11	1038	15
12	137	100	0.73	10,167	0.18	0.0740	0.70	1.7781	1.67	0.1743	1.51	1041	14	1037	11	1036	14
13	102	72.1	0.71	18,709	0.10	0.0732	1.01	1.8026	1.91	0.1785	1.62	1020	20	1046	13	1059	16
14	175	160	0.92	259,896	0.01	0.0746	0.59	1.7851	1.62	0.1734	1.51	1059	12	1040	11	1031	14
15	200	114	0.57	36,519	0.05	0.0741	0.72	1.7950	1.67	0.1756	1.51	1045	15	1044	11	1043	15
16	119	69.1	0.58	32,673	0.06	0.0737	0.70	1.7594	1.69	0.1731	1.53	1034	14	1031	11	1029	15
17	235	251	1.07	82,187	0.02	0.0744	0.42	1.8003	1.57	0.1755	1.51	1052	8	1046	10	1043	15
18	129	97.5	0.76	23,927	0.08	0.0737	0.67	1.7871	1.64	0.1759	1.50	1032	14	1041	11	1045	14

Errors are 1σ; f_{206} is the percentage of common ^{206}Pb in total ^{206}Pb; Common Pb corrected using the measured ^{204}Pb.

Table 2
LA-ICP-MS zircon U-Pb isotopic analyses for the Yuanmou granites in the western Yangtze Block.

Spot	U (ppm)	Th (ppm)	Th/U	$^{206}Pb/^{204}Pb_{measured}$	f_{206} (%)	Isotopic ratio						Age/Ma					
						$^{207}Pb^*/^{206}Pb^*$	± 2σ	$^{207}Pb^*/^{235}U$	± 2σ	$^{206}Pb^*/^{238}U$	± 2σ	$^{207}Pb/^{206}Pb$	± 2σ	$^{207}Pb/^{235}U$	± 2σ	$^{206}Pb/^{238}U$	± 2σ
14YM02-03 (A granitic sample from Yuanmou area: N 25°51′18.4″, E 101°52′24.4″)																	
1	304	98	0.32			0.0724	0.0011	1.6980	0.0340	0.1699	0.0027	1002	30	1007	13	1011	15
2	206	144	0.70			0.0737	0.0020	1.7670	0.0460	0.1745	0.0032	1040	55	1036	18	1037	18
3	417	159	0.38			0.0771	0.0015	1.7700	0.0350	0.1652	0.0027	1129	39	1034	13	986	15
4	367	96	0.26			0.0740	0.0013	1.6650	0.0430	0.1638	0.0029	1037	35	997	16	978	16
5	319	157	0.49			0.0738	0.0018	1.6150	0.0530	0.1605	0.0042	1052	51	977	22	959	24
6	225	169	0.75			0.0763	0.0015	1.7740	0.0410	0.1680	0.0028	1103	38	1035	15	1001	15
7	641	630	0.98			0.0738	0.0011	1.5770	0.0380	0.1553	0.0027	1036	30	960	15	930	15
8	476	195	0.41			0.0730	0.0013	1.7350	0.0560	0.1717	0.0045	1012	35	1020	21	1021	25
9	350	531	1.52			0.0738	0.0022	1.6730	0.0560	0.1646	0.0034	1039	56	997	22	982	19
10	288	208	0.72			0.0739	0.0018	1.6870	0.0510	0.1663	0.0037	1041	51	1002	19	991	20
11	241	187	0.78			0.0736	0.0018	1.6170	0.0460	0.1596	0.0030	1044	47	980	19	954	17
12	352	254	0.72			0.0734	0.0017	1.7270	0.0510	0.1700	0.0041	1029	45	1018	19	1012	22
13	235	74	0.31			0.0753	0.0018	1.8020	0.0490	0.1750	0.0042	1068	47	1045	18	1039	23
14	311	47	0.15			0.0745	0.0012	1.7200	0.0360	0.1700	0.0029	1049	34	1017	13	1012	16
15	214	76	0.36			0.0735	0.0021	1.7410	0.0470	0.1719	0.0042	1016	56	1026	19	1022	23
16	301	193	0.64			0.0756	0.0027	1.7850	0.0710	0.1754	0.0037	1076	74	1039	26	1042	20
17	264	283	1.07			0.0735	0.0013	1.6640	0.0430	0.1630	0.0029	1033	36	994	16	974	16
18	316	69	0.22			0.0743	0.0012	1.7110	0.0350	0.1684	0.0027	1043	32	1012	13	1003	15
19	240	70	0.29			0.0749	0.0012	1.8140	0.0400	0.1766	0.0028	1062	32	1049	15	1048	15

No common lead is corrected.

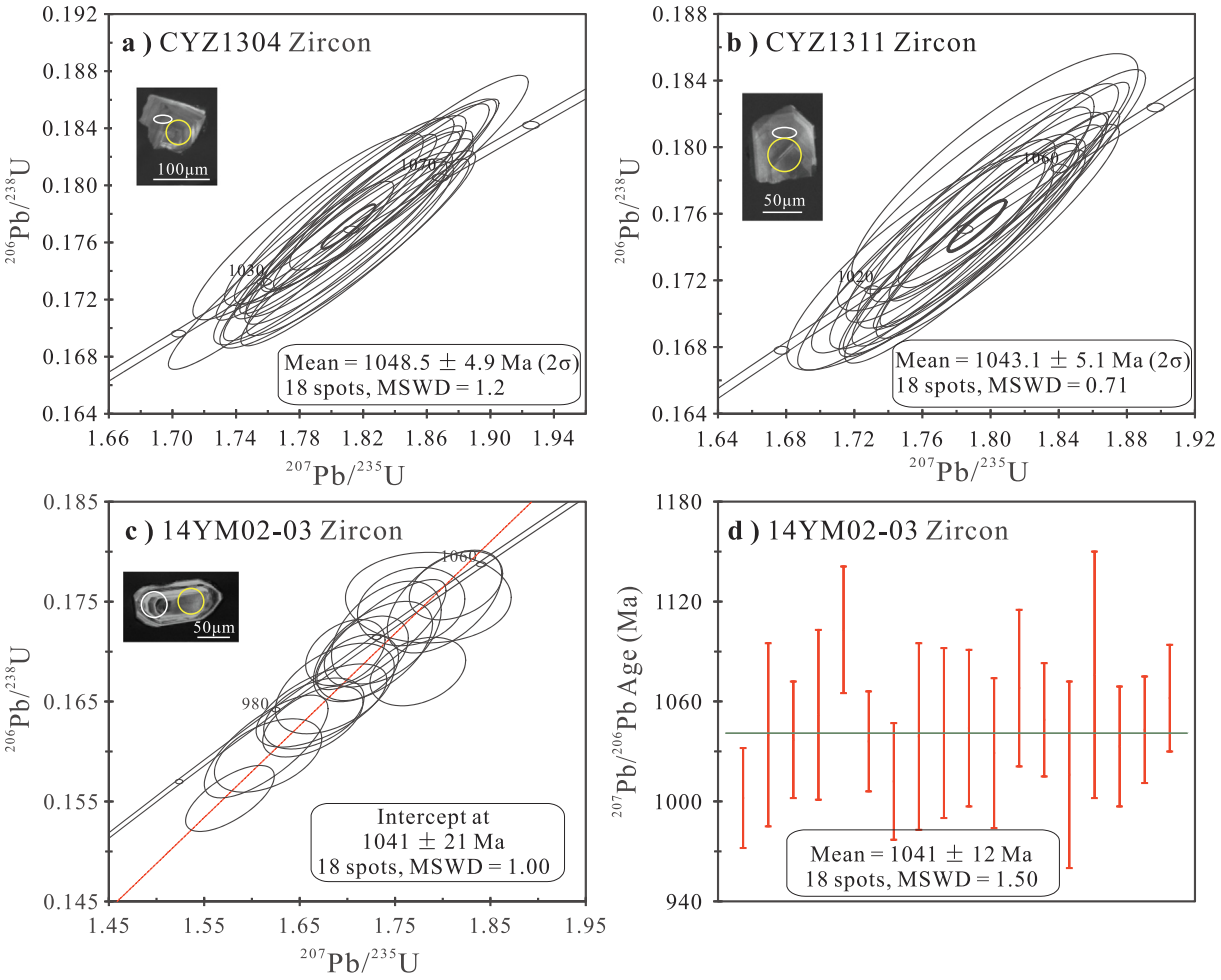

Fig. 3. U-Pb concordia diagrams of zircons from the Huidong (a, b; SIMS) and Yuanmou (c, d; LA-ICP-MS) granites. Also shown are typical zircon CL images with location for laser pits (white circles for U-Pb ages and yellow circles for Lu-Hf measurements) or SIMS pits (white ellipses for U-Pb dating/O isotopic analyses). (For interpretation of the references to color in this figure legend, the reader is referred to the web version of this article.)

Nineteen grains were analyzed by LA-ICP-MS. All analyses show homogenous U (206–641 ppm) and Th (47–630 ppm) contents, with U/Th ratios varying from 0.15 to 1.52. Zircons appear to have experienced variable degrees of lead loss in the conventional Concordia plot (Fig. 3c). Except for #3 which gives an older $^{207}Pb/^{206}Pb$ age of 1129 Ma, all other 18 analyses define a single group with a weighted mean $^{207}Pb/^{206}Pb$ age of 1041 ± 12 Ma (2σ, MSWD = 1.50) (Fig. 3d), same as the intercepted age of 1041 ± 21 Ma (2σ, MSWD = 1.00).

4.2. Whole-rock geochemistry and zircon Hf-O isotopic characteristics

4.2.1. Major and trace elements

Whole-rock major and trace element data for the Huidong and Yuanmou granites are given in Table 3. The Huidong granite samples are characterized by high SiO_2 (72.5–79.5 wt%, volatile free), $Fe_2O_3^T$ (1.8–9.1 wt%), and Al_2O_3 (9.7–12.9 wt%), with low contents of other major oxides, such as MgO (0.1–0.8 wt%), TiO_2 (0.2–0.6 wt%), CaO (0.04–1.4 wt%), K_2O (0.8–5.0 wt%) and P_2O_5 (< 0.02 wt%) (Fig. 4). Except for sample CYZ1302 (4.53 wt%) and CYZ1424 (5.02 wt%), most Huidong granite samples have a narrow range of $Na_2O + K_2O$ at 6.07–7.49 wt%. The Yuanmou granites show similar ranges of SiO_2 (72.2–75.2 wt%), TiO_2 (0.3–0.4 wt%) and $Na_2O + K_2O$ (6.68–8.12 wt%), but higher contents of MgO (0.3–0.6 wt%), CaO (0.3–1.5 wt%), Al_2O_3 (13.4–14.9 wt%) and P_2O_5 (0.1–0.2 wt%), and lower concentrations of $Fe_2O_3^T$ (2.3–3.3 wt%) (Fig. 4). The Huidong and Yuanmou granites are plotted in the sub-alkalic granites field in the total alkali versus silica (TAS) diagram (Fig. 5a). The Huidong granite samples are dominantly metaluminous and peraluminous with A/CNK varying from 1.03 to 1.25 (Fig. 5b). A couple of samples have anomalously high A/CNK value at 1.62–1.78, corresponding with low total alkali and high L.O.I. values, which is likely a result of alteration. The Yuanmou granite samples are mostly peraluminous with A/CNK ranging from 1.15 to 1.26 (Fig. 5b).

The Huidong granite samples are extremely enriched in HFSEs (high field strength elements, e.g., Zr and Nb) and depleted in LILEs (large ion lithosphile elements, e.g., Rb, Sr and Ba) as compared with other granites (Fig. 4). In the primitive-mantle-normalized spider diagram, the Huidong samples are featured with significant negative anomalies in Ba, Sr, Eu and Ti (Fig. 6a). However, their Nb and Ta are only slightly depleted (Nb/La_{PM} = 0.41–2.17, Nb/Th_{PM} = 0.48–1.64). For comparison, the Yuanmou rocks show less significant anomalies in Ba, Sr, Eu and Ti, but more pronounced negative anomalies in Nb-Ta (Nb/La_{PM} = 0.37–0.47, Nb/Th_{PM} = 0.13–0.16) (Fig. 6b). Both Huidong and Yuanmou granites show moderate enrichment (La/Sm_N = 2.2–4.4) in light rare earth elements (LREE) in chondrite-normalized distribution pattern and moderate Eu negative anomaly (Eu/Eu^* = 0.39–0.54) (Fig. 6c, d). The Huidong granites contain 463–2051 ppm total REE, higher than that of the Yuanmou granites (224–345 ppm).

4.2.2. Nd-Hf-O isotopes

Whole-rock Nd and zircon Hf isotopic data are presented in Tables 4 and 5, respectively. Twelve Nd isotopic analyses of the Huidong

Table 3
Major element (wt. %) and trace element (ppm) data for the Huidong and Yuanmou granites in the western Yangtze Block.

Rocks Sample	Huidong K-feldspar granites												
	CYZ1301	CYZ1303	CYZ1304	CYZ1305	CYZ1307	CYZ1308	CYZ1309	CYZ1311	CYZ1315	CYZ 1425	CYZ 1426	CYZ 1428	CYZ1639
SiO_2	78.40	74.80	73.30	72.70	74.10	74.30	74.80	74.00	69.20	73.20	73.60	73.30	73.12
TiO_2	0.28	0.28	0.27	0.40	0.16	0.29	0.20	0.29	0.63	0.24	0.19	0.38	0.31
Al_2O_3	11.15	10.95	11.25	10.70	10.65	10.55	10.98	11.20	12.85	10.75	9.54	10.75	10.84
Fe_2O_3	1.80	5.35	6.22	7.56	6.45	5.85	4.98	5.15	6.82	5.97	8.53	6.96	7.04
MnO	0.02	0.02	0.02	0.02	0.04	0.02	0.01	0.03	0.30	0.03	0.03	0.02	0.03
MgO	0.17	0.05	0.07	0.08	0.17	0.10	0.12	0.23	0.23	0.13	0.15	0.08	0.16
CaO	0.04	0.04	0.06	0.07	0.30	0.09	0.05	0.35	0.14	0.37	0.09	0.06	0.08
Na_2O	4.02	3.21	3.80	3.28	5.27	3.11	3.08	2.76	5.45	3.62	2.64	3.08	3.33
K_2O	2.72	4.08	3.83	3.70	0.75	4.28	4.12	4.11	1.86	3.66	3.31	3.69	3.23
P_2O_5	< 0.01	0.01	0.01	0.01	0.01	< 0.01	0.01	0.01	0.07	0.01	< 0.01	0.01	0.01
LOI	0.79	0.59	0.50	0.60	1.51	0.41	0.65	0.93	1.48	0.84	0.71	0.80	1.28
Total	99.39	99.38	99.33	99.12	99.41	99.00	99.00	99.06	99.03	98.82	98.79	99.13	99.43
A/CNK	1.16	1.12	1.07	1.12	1.06	1.06	1.14	1.16	1.14	1.02	1.18	1.17	1.19
Sc	1.47	1.60	1.52	6.39	8.25	1.38	5.80	8.11	12.9	7.04	6.79	2.50	4.95
V	1.10	2.70	2.17	2.97	4.01	2.12	5.02	2.56	4.12	4.40	1.87	3.34	1.45
Co	1.35	1.20	1.20	1.00	5.25	1.84	1.05	1.08	3.89	0.52	2.00	1.12	1.71
Cu	16.1	39.1	17.1	72.0	59.3	7.20	21.3	11.1	4.77	35.0	42.6	99.7	40.1
Zn	11.5	18.1	22.5	50.3	66.8	22.6	60.9	43.9	46.6	68.8	84.2	51.0	30.2
Ga	53.5	46.8	46.9	44.8	42.9	47.3	39.3	44.5	36.1	43.0	48.0	43.4	44.3
Rb	37.7	65.0	57.7	47.4	22.7	40.7	50.6	64.1	42.0	48.4	44.7	47.5	43.4
Sr	5.34	5.38	5.39	9.43	10.7	7.68	6.68	8.27	20.6	8.51	7.69	8.31	6.80
Y	174	173	252	180	123	226	141	210	188	202	218	193	190
Zr	2046	2135	1946	1410	1360	1753	1420	1750	1850	1750	1690	1640	1570
Nb	191	162	183	136	86.7	166	96	187	106	118	161	135	134
Cs	0.36	0.48	0.34	0.30	0.15	0.17	0.28	0.78	0.41	0.14	0.34	0.29	0.43
Ba	148	291	235	352	188	263	280	374	417	265	251	305	271
La	452	72.0	217	127	97.7	304	89.0	137	67.8	141	73.3	113	176
Ce	885	155	470	233	175	592	168	363	103	304	206	275	308
Pr	103	20.3	58.9	31.8	23.3	67.8	24.4	34.6	18.6	36.0	19.8	31.9	46.8
Nd	383	80.7	236	131	95.9	269	98.2	143	80.7	144	82.2	133	196
Sm	65.0	18.3	47.2	28.3	20.5	50.8	19.4	31.0	19.4	29.9	19.6	28.3	40.7
Eu	7.95	3.11	6.80	4.55	3.36	7.90	3.05	4.98	4.68	4.82	3.13	4.87	7.22
Gd	51.4	20.6	44.1	26.6	20.6	50.5	18.5	32.3	24.2	29.2	22.9	27.3	41.4
Tb	6.47	4.29	7.72	5.15	3.52	7.64	3.58	6.21	4.98	5.64	4.98	5.41	6.66
Dy	36.9	30.8	50.4	32.3	21.8	44.9	25.1	38.9	31.7	35.2	36.2	34.2	37.6
Ho	7.93	7.14	10.9	6.82	4.73	9.49	5.63	8.72	7.01	7.60	8.51	7.46	7.35
Er	22.8	21.4	30.7	21.6	15.0	25.7	17.1	26.3	20.6	22.6	26.2	22.7	21.6
Tm	3.55	3.43	4.56	3.35	2.24	3.85	2.52	3.81	3.18	3.46	4.27	3.41	3.01
Yb	23.4	23.2	28.7	22.4	16.0	24.8	16.8	24.9	20.9	22.0	28.5	21.8	19.9
Lu	3.55	3.61	4.22	3.47	2.51	3.71	2.40	3.63	3.22	3.28	4.24	3.13	2.84
Hf	48.4	50.4	46.6	33.0	34.3	42.5	34.2	42.2	37.6	41.4	39.5	37.0	41.7
Ta	11.5	10.7	11.1	7.37	4.91	9.97	5.50	10.4	5.75	6.83	9.48	7.32	8.77
Pb	4.14	2.95	3.00	5.28	3.87	3.75	4.02	6.75	5.07	3.70	4.11	5.11	3.85
Th	47.3	28.4	34.9	25.4	15.2	32.7	20.2	35.3	19.9	25.4	34.9	26.7	26.5
U	7.82	7.30	7.64	5.09	3.53	6.59	4.35	6.91	4.11	5.79	6.85	5.11	4.75
T_{Zr}	1139	1129	1092	1048	1031	1077	1060	1101	1086	1060	1100	1089	1084

Rocks Sample	Huidong K-feldspar granites					Yuanmou biotite granites						
	CYZ1640	CYZ1641	CYZ1302	CYZ1314	CYZ1424	14YM02-1	14YM02-2	14YM02-3	14YM02-4	14YM02-5	14YM02-6	14YM02-7

(*continued on next page*)

Table 3 (*continued*)

Rocks Sample	Huidong K-feldspar granites					Yuanmou biotite granites						
	CYZ1640	CYZ1641	CYZ1302	CYZ1314	CYZ1424	14YM02-1	14YM02-2	14YM02-3	14YM02-4	14YM02-5	14YM02-6	14YM02-7
SiO_2	72.95	74.43	72.20	70.80	74.60	72.29	72.73	73.10	70.75	74.00	71.64	72.39
TiO_2	0.30	0.17	0.58	0.59	0.24	0.30	0.39	0.26	0.42	0.25	0.28	0.30
Al_2O_3	11.27	10.16	10.21	12.55	9.60	13.88	13.20	13.68	14.52	13.78	13.81	13.48
Fe_2O_3	6.43	6.25	8.79	4.95	7.55	3.01	3.17	2.49	3.20	2.26	3.16	3.11
MnO	0.03	0.02	0.03	0.16	0.03	0.02	0.02	0.02	0.04	0.02	0.03	0.02
MgO	0.11	0.10	0.80	0.20	0.44	0.61	0.61	0.53	0.53	0.38	0.31	0.62
CaO	0.18	0.06	0.08	1.37	0.04	0.49	0.41	0.43	1.42	0.72	0.96	0.33
Na_2O	3.86	2.98	2.49	6.86	0.07	2.78	3.21	2.94	3.69	4.16	2.90	3.17
K_2O	3.22	4.15	1.91	0.19	4.82	5.11	4.81	5.03	2.82	2.65	5.03	4.56
P_2O_5	0.01	0.01	0.02	0.02	0.01	0.15	0.20	0.16	0.13	0.17	0.17	0.16
LOI	0.75	0.74	1.92	1.77	1.63	1.15	0.87	1.06	2.12	1.43	1.31	1.32
Total	99.11	99.07	99.03	99.46	99.03	99.79	99.62	99.70	99.64	99.82	99.60	99.46
A/CNK	1.11	1.07	1.62	0.90	1.78	1.26	1.18	1.24	1.24	1.25	1.15	1.25
Sc	4.45	4.00	6.26	17.5	4.72	7.18	8.85	8.03	13.7	7.12	5.86	6.88
V	0.68	1.18	2.28	9.33	3.83	16.7	19.1	16.3	27.3	14.6	15.7	17.2
Co	2.15	2.76	6.38	4.63	1.11	2.33	2.91	2.81	3.55	2.93	2.53	2.65
Cu	28.4	5.50	29.5	340	3.73	3.34	5.32	3.56	12.2	23.4	4.54	6.73
Zn	37.1	31.5	73.2	46.7	99.7	17.5	15.9	19.4	19.8	13.7	446	16.7
Ga	45.1	40.6	44.9	43.0	46.3	26.3	24.3	29.9	29.5	25.8	26.3	26.5
Rb	38.5	39.3	34.6	5.8	114	183	158	198	118	92.9	180	157
Sr	5.99	6.82	8.52	11.9	5.48	85.0	80.7	101	235	220	120	79.5
Y	169	184	282	141	150	49.6	66.3	69.2	82.2	61.7	66.0	57.6
Zr	1530	1530	2330	1210	1440	261	352	272	369	257	276	293
Nb	136	172	199	142	108	21.4	25.2	22.1	23.8	17.1	21.8	22.3
Cs	0.17	0.24	0.44	0.14	1.72	3.31	2.90	3.88	3.47	1.58	4.09	2.82
Ba	321	336	116	126	269	655	712	750	924	674	784	610
La	165	117	173	138	71.7	44.8	66.2	52.9	57.7	42.4	46.5	45.4
Ce	249	264	351	264	202	93.7	134	108	112	83.6	96.5	95.3
Pr	40.2	31.7	51.5	36.9	19.8	11.2	17.1	13.1	14.0	10.4	11.8	11.6
Nd	167	134	218	154	81.1	44.3	64.3	50.4	55.0	39.8	45.2	46.0
Sm	34.2	29.8	50.0	29.5	17.0	10.1	14.6	11.9	11.9	9.53	10.7	11.2
Eu	5.92	5.04	8.59	4.28	2.51	1.36	1.86	1.72	1.78	1.35	1.63	1.40
Gd	35.5	31.1	48.9	29.9	16.1	9.52	13.0	11.7	11.7	8.97	11.2	10.7
Tb	5.81	5.76	9.24	4.89	3.20	1.67	2.31	2.13	2.22	1.79	2.06	1.95
Dy	33.6	37.4	58.6	26.6	23.5	9.66	13.7	12.9	14.4	11.1	12.5	11.8
Ho	6.69	7.84	12.5	5.49	5.64	1.77	2.57	2.55	3.00	2.12	2.36	2.15
Er	20.3	24.4	36.5	16.2	19.1	4.98	7.21	6.99	9.15	6.25	6.73	5.88
Tm	2.88	3.61	5.22	2.39	3.36	0.68	1.00	0.98	1.41	0.80	0.99	0.81
Yb	18.9	24.2	34.2	15.8	23.9	3.95	5.88	5.88	8.71	4.91	5.97	4.88
Lu	2.79	3.57	5.16	2.45	3.70	0.57	0.78	0.86	1.31	0.75	0.87	0.62
Hf	41.2	41.2	54.0	28.2	34.1	7.05	9.67	7.38	9.40	6.67	7.04	7.68
Ta	8.77	10.9	11.3	6.63	7.91	1.40	1.89	1.54	1.32	1.39	1.54	1.50
Pb	3.44	3.93	3.71	4.39	3.75	20.3	19.1	23.3	7.97	11.0	24.6	15.2
Th	22.6	31.2	29.6	10.3	26.5	15.9	21.8	19.3	19.2	16.1	17.6	17.7
U	5.16	6.25	6.92	6.30	4.19	4.77	5.73	5.21	3.27	2.74	4.67	5.36
T_{Zr}	1059	1056	1240	950	1164	825	850	828	862	824	816	838

A/CNK = molar $Al_2O_3/(CaO + Na_2O + K_2O)$; Total iron as Fe_2O_3; LOI = loss on ignition; T_{Zr}: zircon saturation temperatures according to Boehnke et al. (2013).

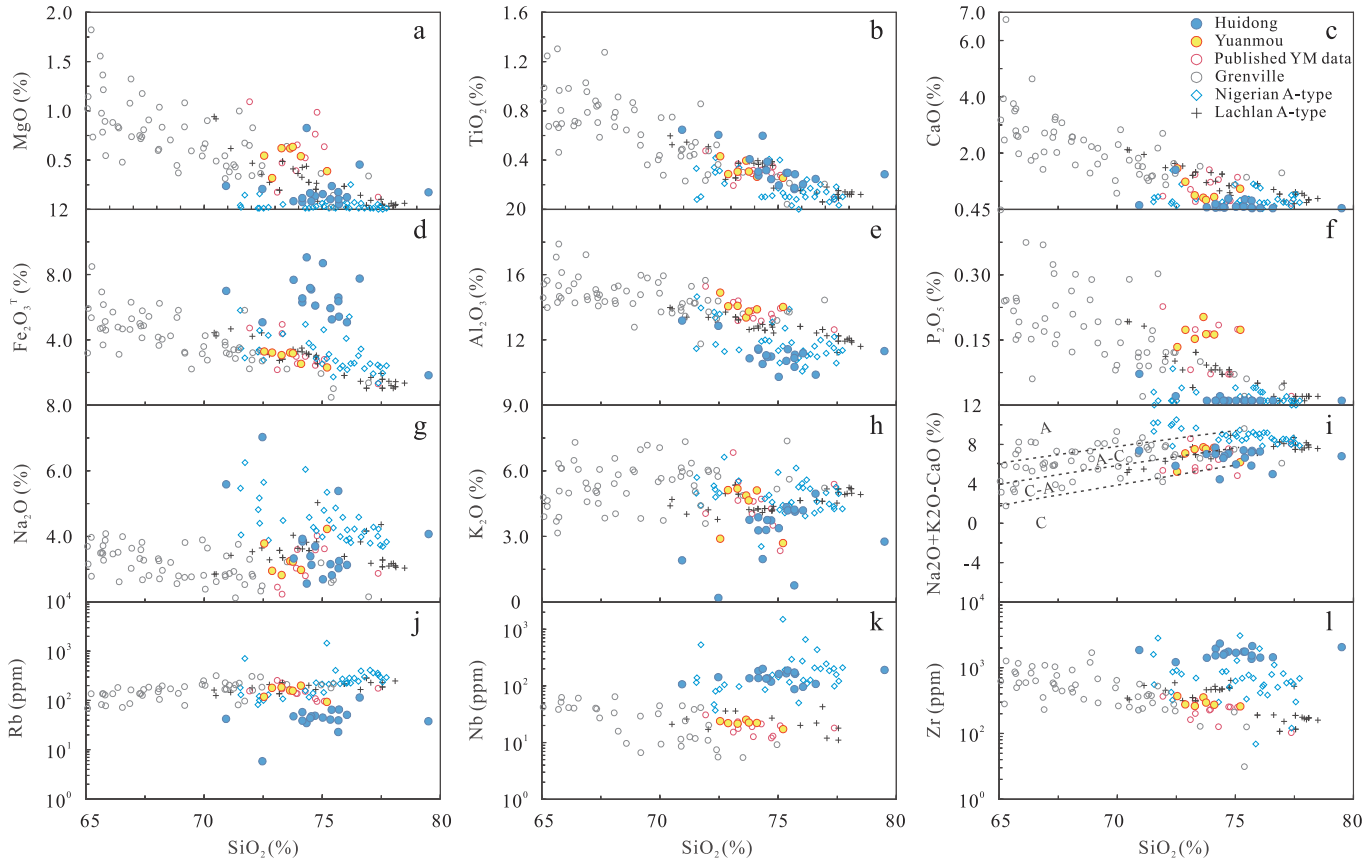

Fig. 4. Selected variation diagrams of major oxides and trace element contents versus silica for the Huidong and Yuanmou granites. Also shown is data from the Grenville province, Nigeria, and Lachlan belt.

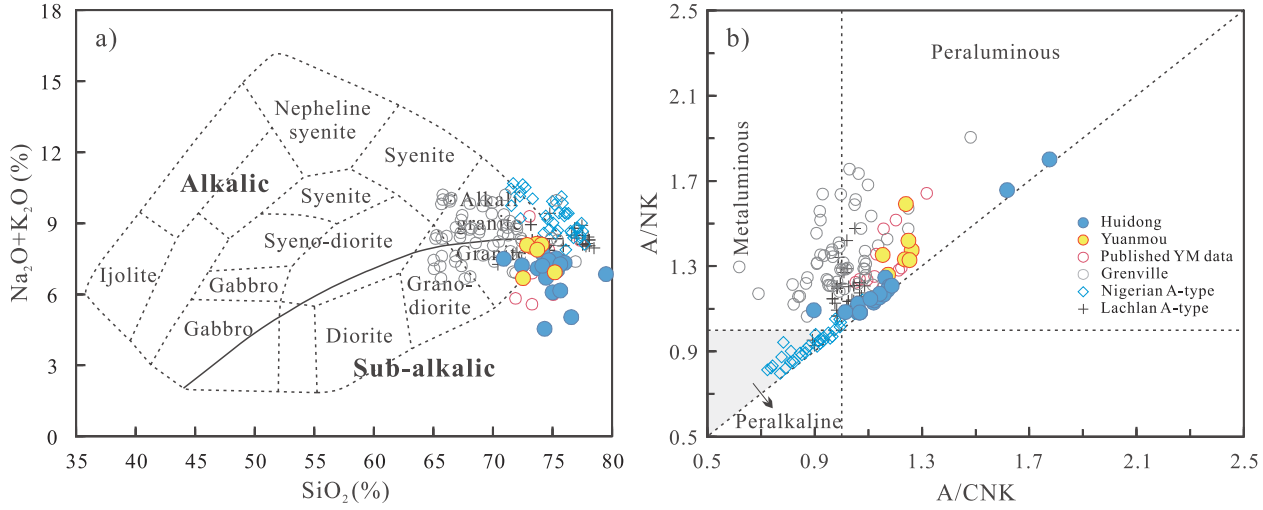

Fig. 5. (a) Plots of SiO_2 vs. (Na_2O + K_2O) (Cox et al., 1979) and (b) A/NK vs. A/CNK showing the meta-peraluminous nature of the Yuanmou and Huidong granites. A/CNK = Al_2O_3/(CaO + Na_2O + K_2O) molar, A/NK = Al_2O_3/(Na_2O + K_2O) molar.

granites yield variable $^{147}Sm/^{144}Nd$ ratios (0.1091–0.1431) and $^{143}Nd/^{144}Nd$ ratios (0.512110–0.512373). These samples have high initial $\varepsilon_{Nd}(t = 1040\ Ma)$ from +0.58 to +4.4, similar to coeval mafic rocks in the region (bold values in Table 4; Fig. 7a). 46 analyses of Hf isotopes on zircons of the Huidong granites show a range of $\varepsilon_{Hf}(t)$ from +6.0 to +8.3, and T^{Hf}_{2DM} of 1.36–1.50 Ga (Table 5; Fig. 7b). The Yuanmou granite samples have $^{147}Sm/^{144}Nd$ ratios and $^{143}Nd/^{144}Nd$ ratios ranging from 0.1232 to 0.1478 and 0.512161–0.512210, respectively. Their initial $\varepsilon_{Nd}(t = 1040\ Ma)$ values range from −2.0 to +0.59 (Table 4; Fig. 7a). Similarly, their zircon $\varepsilon_{Hf}(t)$ values (−1.5 to +5.1) are also lower than the Huidong granites, and correspond with an older T^{Hf}_{2DM} from 1.56 to 1.97 Ga (Table 5; Fig. 7b).

Thirty-eight $\delta^{18}O$ analyses on zircons of the Huidong granites yield a narrow range of 6.2–7.2 ‰, slightly higher than the ~5.3 ± 0.6‰ of magmatic zircons from mantle, but much lower than the values of typical S-type granites (Table 6; Fig. 8).

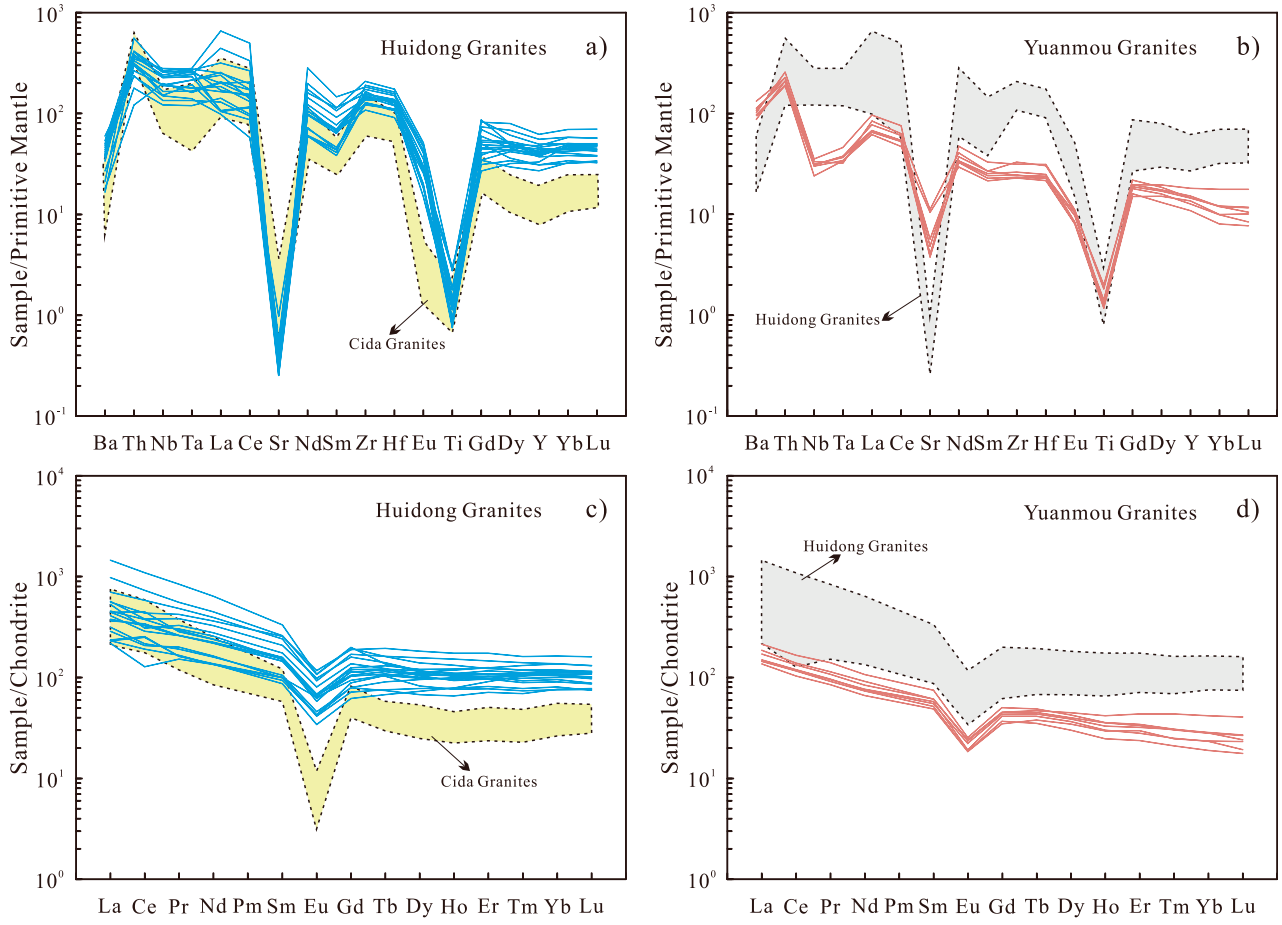

Fig. 6. Primitive mantle-normalized incompatible trace element multi-element plots and chondrite-normalized REE diagrams for the Huidong granites (a, c) and the Yuanmou granites (b, d). Chondrite-normalizing values are from Boynton (1984). Primitive mantle-normalizing values are from Sun and McDonough (1989). Data of the highly-evolved mantle-derived Cida granites associated with ELIP magmatism come from Zhong et al. (2007).

5. Discussion

5.1. Geochronology

New zircon U-Pb dating results suggest that the Huidong and Yuanmou granites were emplaced contemporaneously at 1041–1049 Ma, indistinguishable from the ages of Julin meta-basalts and granitic rocks (ca. 1050 Ma; '3' in Fig. 1b), and are only slightly older than ~1020 Ma mafic dykes and intermediate and felsic volcanic rocks in the Huili area ('4' and '5' in Fig. 1b). Interestingly, the ages are also similar to those of granitoids in Grenville orogen of North America. For instance, ~450 km^2 Saint-Urbain AMCG suite was dated at 1046–1055 Ma in the Château-Richer-Saint-Urbain–Mattawa–Labrieville (CRUML) belt (Morisset et al., 2009), coeval with the 1060–1040 Ma Lyon Mountain Gneiss (McLelland et al., 2001). Ca. 1060 Ma Havre-Saint-Pierre AMCG suite, numerous 1080–1010 Ma

Table 4
Whole-rock Sm-Nd isotopic data for the Huidong and Yuanmou granites in the western Yangtze Block.

	Sample No.	Age (Ma)	Sm (ppm)	Nd (ppm)	$^{147}Sm/^{144}Nd$	$^{143}Nd/^{144}Nd$	(2σ)	$(^{143}Nd/^{144}Nd)_I$	$\varepsilon_{Nd}(T)$	T_{DM} (Ga)	T_{2DM}(Ga)
HuidongK-feldspar granites	CYZ1301	1040	65.8	365	0.1091	0.512110	0.000009	0.511365	**1.36**	1.35	1.39
	CYZ1303	1040	16.9	71.5	0.1431	0.512302	0.000010	0.511325	**0.58**	1.57	1.42
	CYZ1304	1040	50.6	238	0.1284	0.512265	0.000011	0.511388	**1.81**	1.38	1.34
	CYZ1305	1040	27.0	140	0.1162	0.512311	0.000018	0.511518	**4.35**	1.16	1.16
	CYZ1308	1040	48.5	242	0.1212	0.512235	0.000011	0.511408	**2.20**	1.33	1.32
	CYZ1309	1040	21.4	103	0.1254	0.512243	0.000012	0.511387	**1.78**	1.37	1.35
	CYZ1311	1040	32.1	141	0.1371	0.512277	0.000011	0.511341	**0.89**	1.50	1.40
	CYZ1312	1040	86.4	418	0.1250	0.512333	0.000004	0.511481	**3.62**	1.22	1.21
	CYZ1314	1040	32.1	153	0.1270	0.512221	0.000012	0.511354	**1.15**	1.43	1.39
	CYZ1425	1040	30.4	133	0.1378	0.512316	0.000020	0.511375	**1.56**	1.44	1.36
	CYZ1428	1040	29.4	130	0.1372	0.512343	0.000019	0.511407	**2.18**	1.38	1.31
	CYZ1641	1040	30.6	130	0.1419	0.512373	0.000015	0.511404	**2.12**	1.41	1.31
Yuanmou biotite granites	14YM02-1	1040	9.69	47.0	0.1247	0.512177	0.000021	0.511326	**0.59**	1.47	1.43
	14YM02-2	1040	14.2	69.5	0.1232	0.512161	0.000020	0.511320	**0.48**	1.47	1.44
	14YM02-6	1040	11.0	45.2	0.1478	0.512204	0.000016	0.511195	**−1.97**	1.86	1.60
	14YM02-7	1040	10.5	46.0	0.1374	0.512210	0.000026	0.511272	**−0.45**	1.63	1.50

T_{DM} and T_{2DM} represent calculated one and two-stage model ages, respectively.

Table 5
Zircon Hf isotopic composition for the Huidong and Yuanmou granites in the western Yangtze Block.

	No.	$^{176}Yb/^{177}Hf$	$^{176}Lu/^{177}Hf$	1σ	$^{176}Hf/^{177}Hf$	1σ	Age (Ma)	ε_{Hf} (t)	T_{DM1} (Ga)	T_{DM2} (Ga)
Huidong Granites	CYZ1304-01	0.077958	0.002447	0.000033	0.282376	0.000017	1040	7.34	1.29	1.42
	CYZ1304-02	0.063124	0.002073	0.000012	0.282353	0.000018	1040	6.77	1.31	1.45
	CYZ1304-03	0.090216	0.002946	0.000040	0.282380	0.000017	1040	7.14	1.30	1.43
	CYZ1304-04	0.069949	0.002236	0.000020	0.282361	0.000021	1040	6.96	1.30	1.44
	CYZ1304-05	0.096628	0.003090	0.000026	0.282352	0.000017	1040	6.04	1.35	1.50
	CYZ1304-06	0.102174	0.003239	0.000034	0.282394	0.000017	1040	7.44	1.29	1.41
	CYZ1304-07	0.076434	0.002516	0.000014	0.282357	0.000017	1040	6.60	1.32	1.46
	CYZ1304-08	0.079128	0.002482	0.000014	0.282369	0.000018	1040	7.08	1.30	1.43
	CYZ1304-09	0.129441	0.003370	0.000029	0.282398	0.000022	1040	7.49	1.29	1.41
	CYZ1304-10	0.108050	0.002902	0.000056	0.282386	0.000017	1040	7.39	1.29	1.41
	CYZ1304-11	0.133388	0.003506	0.000002	0.282410	0.000024	1040	7.80	1.27	1.39
	CYZ1304-12	0.095291	0.002481	0.000016	0.282366	0.000020	1040	6.95	1.30	1.44
	CYZ1304-13	0.111133	0.003072	0.000038	0.282395	0.000017	1040	7.59	1.28	1.40
	CYZ1304-14	0.139133	0.003602	0.000003	0.282425	0.000018	1040	8.26	1.26	1.36
	CYZ1304-15	0.105717	0.002808	0.000043	0.282365	0.000018	1040	6.69	1.32	1.46
	CYZ1304-16	0.112098	0.002969	0.000025	0.282368	0.000018	1040	6.68	1.32	1.46
	CYZ1304-17	0.121702	0.003241	0.000003	0.282386	0.000018	1040	7.15	1.30	1.43
	CYZ1304-18	0.106486	0.002916	0.000035	0.282380	0.000018	1040	7.15	1.30	1.43
	CYZ1304-19	0.104482	0.002718	0.000006	0.282376	0.000017	1040	7.13	1.30	1.43
	CYZ1304-20	0.112180	0.002977	0.000026	0.282390	0.000017	1040	7.47	1.28	1.41
	CYZ1304-21	0.117896	0.003222	0.000024	0.282392	0.000017	1040	7.36	1.29	1.42
	CYZ1304-22	0.109516	0.003016	0.000009	0.282378	0.000018	1040	7.01	1.30	1.44
	CYZ1304-23	0.121554	0.003161	0.000023	0.282383	0.000016	1040	7.10	1.30	1.43
	CYZ1304-24	0.131569	0.003472	0.000002	0.282399	0.000021	1040	7.45	1.29	1.41
	CYZ1304-25	0.124494	0.003279	0.000014	0.282382	0.000017	1040	6.98	1.31	1.44
	CYZ1304-26	0.098363	0.002567	0.000001	0.282357	0.000018	1040	6.56	1.32	1.47
	CYZ1304-27	0.130113	0.003338	0.000016	0.282411	0.000019	1040	7.95	1.27	1.38
	CYZ1311-01	0.114543	0.002949	0.000022	0.282388	0.000020	1040	7.42	1.29	1.41
	CYZ1311-02	0.126164	0.003259	0.000010	0.282387	0.000018	1040	7.16	1.30	1.43
	CYZ1311-03	0.134686	0.003411	0.000001	0.282404	0.000025	1040	7.64	1.28	1.40
	CYZ1311-04	0.110268	0.002867	0.000025	0.282379	0.000020	1040	7.13	1.30	1.43
	CYZ1311-05	0.088587	0.002305	0.000008	0.282368	0.000017	1040	7.17	1.29	1.43
	CYZ1311-06	0.113007	0.002878	0.000025	0.282383	0.000017	1040	7.28	1.29	1.42
	CYZ1311-07	0.110627	0.002959	0.000004	0.282372	0.000018	1040	6.82	1.31	1.45
	CYZ1311-08	0.124444	0.003126	0.000093	0.282386	0.000023	1040	7.23	1.30	1.42
	CYZ1311-09	0.125322	0.003233	0.000039	0.282392	0.000014	1040	7.35	1.29	1.42
	CYZ1311-11	0.089946	0.002399	0.000018	0.282354	0.000015	1040	6.60	1.32	1.46
	CYZ1311-10	0.066061	0.001743	0.000016	0.282363	0.000013	1040	7.37	1.28	1.41
	CYZ1311-12	0.080808	0.002099	0.000012	0.282394	0.000020	1040	8.22	1.25	1.36
	CYZ1311-13	0.120214	0.003035	0.000005	0.282391	0.000031	1040	7.45	1.29	1.41
	CYZ1311-14	0.078719	0.002093	0.000013	0.282347	0.000019	1040	6.54	1.32	1.47
	CYZ1311-15	0.075120	0.002023	0.000067	0.282358	0.000020	1040	7.00	1.30	1.44
	CYZ1311-16	0.083232	0.002409	0.000019	0.282343	0.000020	1040	6.18	1.33	1.49
	CYZ1311-17	0.077507	0.002142	0.000013	0.282365	0.000019	1040	7.15	1.29	1.43
	CYZ1311-18	0.072933	0.002100	0.000038	0.282371	0.000018	1040	7.40	1.28	1.41
	CYZ1311-19	0.066620	0.001885	0.000011	0.282340	0.000015	1040	6.46	1.32	1.47
Yuanmou Granites	14YM02-1	0.034674	0.000856	0.000011	0.282207	0.000017	1040	2.46	1.47	1.72
	14YM02-2	0.040096	0.001051	0.000024	0.282138	0.000025	1040	−0.14	1.57	1.89
	14YM02-3	0.036432	0.001001	0.000029	0.282178	0.000015	1040	1.33	1.51	1.79
	14YM02-4	0.038962	0.001136	0.000040	0.282132	0.000019	1040	−0.39	1.58	1.90
	14YM02-5	0.040538	0.001148	0.000013	0.282136	0.000021	1040	−0.28	1.58	1.89
	14YM02-6	0.047286	0.001354	0.000029	0.282144	0.000020	1040	−0.13	1.58	1.88
	14YM02-7	0.031681	0.000885	0.000024	0.282098	0.000014	1040	−1.45	1.62	1.97
	14YM02-8	0.029111	0.000891	0.000008	0.282108	0.000018	1040	−1.09	1.61	1.94
	14YM02-9	0.071440	0.001960	0.000104	0.282304	0.000018	1040	5.13	1.37	1.56
	14YM02-10	0.062264	0.001744	0.000044	0.282255	0.000024	1040	3.53	1.43	1.66
	14YM02-11	0.048477	0.001246	0.000014	0.282205	0.000012	1040	2.11	1.49	1.74
	14YM02-12	0.033239	0.000960	0.000026	0.282203	0.000016	1040	2.23	1.48	1.74
	14YM02-13	0.023813	0.000680	0.000020	0.282169	0.000027	1040	1.23	1.51	1.80
	14YM02-14	0.044831	0.001313	0.000032	0.282186	0.000032	1040	1.40	1.51	1.79
	14YM02-15	0.049184	0.001222	0.000016	0.282207	0.000014	1040	2.20	1.48	1.74
	14YM02-16	0.048091	0.001368	0.000026	0.282143	0.000014	1040	−0.18	1.58	1.89
	14YM02-17	0.055571	0.001474	0.000020	0.282256	0.000020	1040	3.76	1.42	1.64
	14YM02-18	0.028630	0.000831	0.000014	0.282253	0.000018	1040	4.11	1.40	1.62

T_{DM} and T_{2DM} represent calculated one and two-stage model ages, respectively.

anorthosite and related ~1050 Ma A-type granitoid plutons also occur in the extending areas of the CRUML belt (Morisset et al., 2009; McLelland et al., 2010 and references therein).

5.2. Petrogenesis of the Huidong and Yuanmou granites

Both Huidong and Yuanmou granites have high Ga/Al ratios (3.43–9.33) and are enriched in total $Fe_2O_3^T$ and HFSE but depleted in MgO. These features are distinct from those of I- and S-type granites but are characteristic of A-type granites (Fig. 9). A-type granites may form

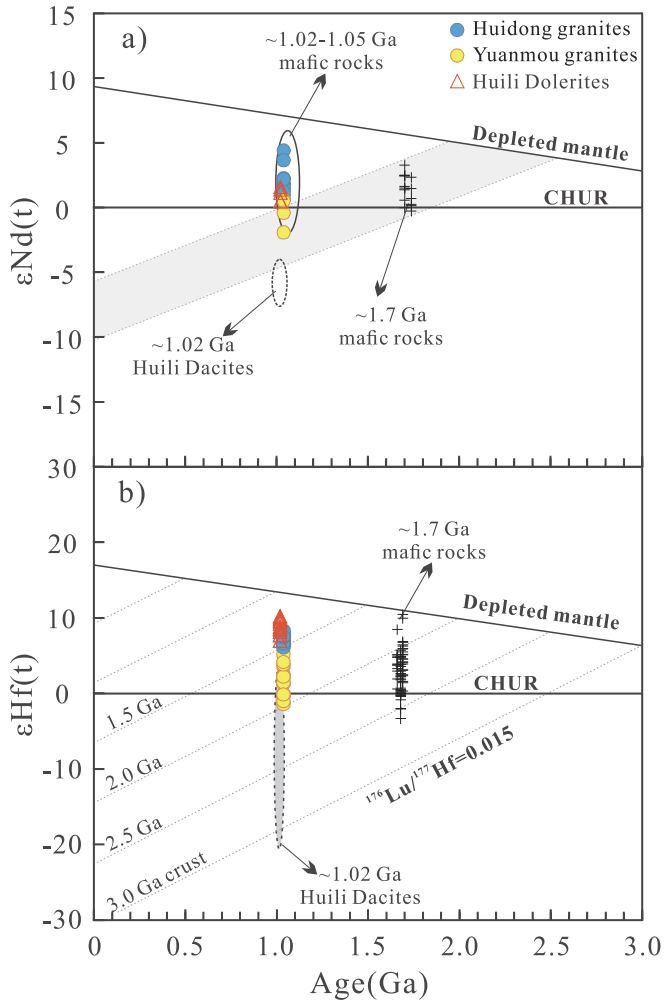

Fig. 7. Plots of whole-rock ε_{Nd} (t) (a) and zircon ε_{Hf} (t) (b) vs. age for the Huidong and Yuanmou granites with regional coeval igneous rocks in the western Yangtze Block. Also shown are Nd-Hf composition of ~1.7 Ga mafic rocks from Zhao et al. (2010), Chen et al. (2013), and Zhu et al. (2017). Data of ~1.05–1.02 Ga regional mafic and felsic rocks are cited from Chen et al. (2014, 2018) and Zhu et al. (2016).

by (1) fractional crystallization of basaltic magmas with or without crustal assimilation (Loiselle and Wones, 1979; Eby, 1990; Turner et al., 1992; Han et al., 1997), (2) partial melting of anhydrous crustal rocks (Collins et al., 1982; Whalen et al., 1987; Frost and Frost, 1997; Huang et al., 2011), or (3) mixing of mantle- and crustal-derived magmas (Kerr and Fryer, 1993; Yang et al., 2007). The remarkable difference in geochemistry and isotopic compositions between the Huidong and Yuanmou granites may suggest contrast in their petrogenesis, which we will explain below.

5.2.1. Petrogenesis of Huidong A-type granites

In general, granitic rocks form by fractionation of basaltic magmas or by crustal melting. Most Huidong samples have high SiO_2 at around 75 wt%. They are extremely depleted in MgO, CaO and Al_2O_3, but enriched in $Fe_2O_3^T$ (Fig. 4). They are also enriched in HFSEs and depleted in LILEs (Figs. 4 and 6). Highly radiogenic Nd–Hf isotopes, low Th/Nb and high Nb/La ratios support the genetic relationship between the Huidong granites and regional coeval mafic magmatism. We consider that the Huidong granites may form through extreme fractional crystallization of tholeiitic magmas. Geochemical modelling using Sr versus Zr and V versus Zr indicates that the high-Si Huidong granites may have formed after 90% fractionation of tholeiitic basalts similar to those outcropped in the region (Fig. 11). The model is similar to that

Table 6
Zircon ^{18}O isotopic composition for the Huidong granites in the western Yangtze Block.

Sample	No.	$\delta^{18}O$ (‰)	2σ
Huidong Granites	CYZ1304-1	6.20	0.26
	CYZ1304-2	6.55	0.47
	CYZ1304-3	6.35	0.33
	CYZ1304-4	6.65	0.34
	CYZ1304-5	6.38	0.28
	CYZ1304-6	6.67	0.26
	CYZ1304-7	6.50	0.38
	CYZ1304-8	6.41	0.28
	CYZ1304-9	6.43	0.30
	CYZ1304-10	6.79	0.42
	CYZ1304-11	6.67	0.37
	CYZ1304-12	6.76	0.25
	CYZ1304-13	6.78	0.44
	CYZ1304-14	6.34	0.30
	CYZ1304-15	6.70	0.25
	CYZ1304-16	6.55	0.24
	CYZ1304-17	6.84	0.41
	CYZ1304-18	6.29	0.34
	CYZ1304-19	6.50	0.30
	CYZ1311-1	7.03	0.29
	CYZ1311-2	7.22	0.37
	CYZ1311-3	6.72	0.24
	CYZ1311-4	6.93	0.33
	CYZ1311-5	6.62	0.25
	CYZ1311-6	6.61	0.31
	CYZ1311-7	6.47	0.30
	CYZ1311-8	6.17	0.34
	CYZ1311-9	6.37	0.28
	CYZ1311-10	6.64	0.22
	CYZ1311-11	6.64	0.28
	CYZ1311-12	6.94	0.18
	CYZ1311-13	6.34	0.48
	CYZ1311-14	6.79	0.31
	CYZ1311-15	6.42	0.36
	CYZ1311-16	6.48	0.26
	CYZ1311-17	6.53	0.39
	CYZ1311-18	6.48	0.28
	CYZ1311-19	6.90	0.32

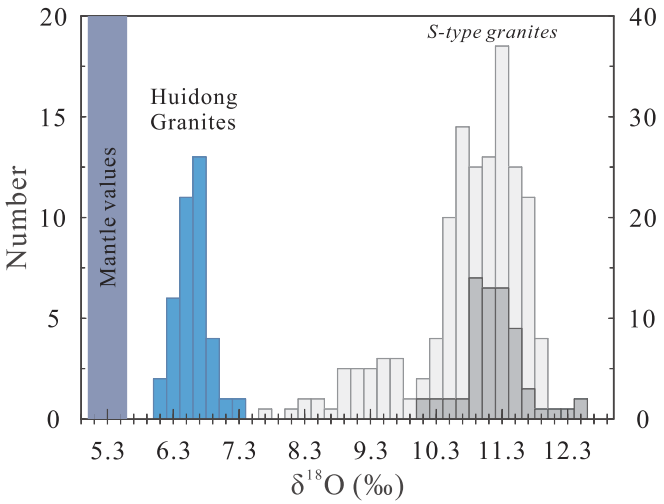

Fig. 8. (a) Histogram of the zircon $\delta^{18}O$ values of the Huidong granites in the western Yangtze Block. Zircon $\delta^{18}O$ data of typical S-type granites (~11.0‰) come from studies of Jeon et al. (2012) (dark grey) and Jiao et al. (2015) (shallow grey). Mantle field is according to Valley et al. (2005).

proposed for ferroan calc-alkalic to calcic metaluminous granitoids such as Thingmuli rhyolites and Skaergaard granophyres (see Frost and Frost, 2011 and references therein). However, numerical modelling by Lee and Bachmann (2014) suggested that high-silica felsic rocks

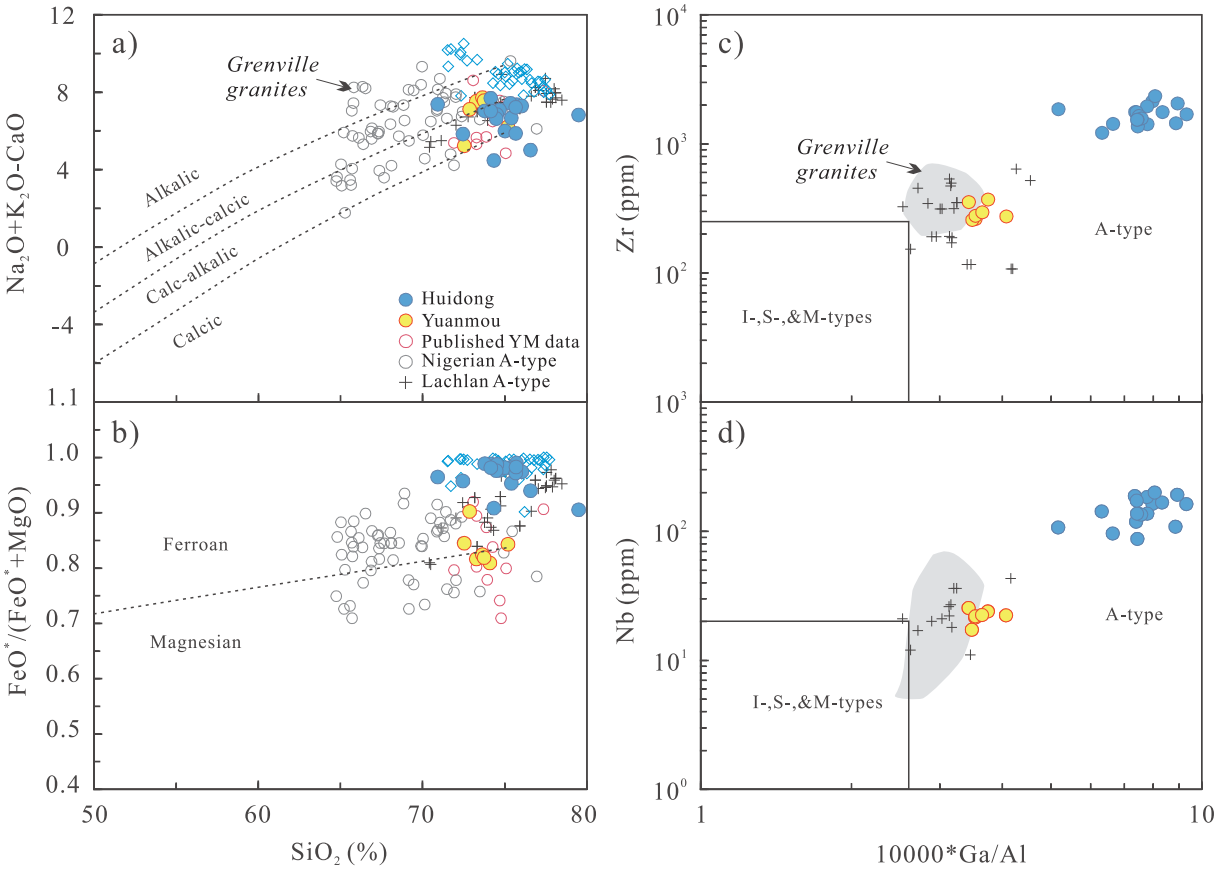

Fig. 9. Geochemical classification diagrams based on MALI (a; Frost et al., 2001), Fe-number (b; Frost et al., 2001) and trace elements (c-d; Whalen et al., 1987) for the Huidong and Yuanmou granites. Also shown is the data from the Lachlan A-type granites (Collins et al., under review and references therein) and granitoids in Grenville province (Higgins and Breemen, 1996; Gorring et al., 2004; Hughes et al., 2004; Tollo et al., 2004; Quinn, 2012).

(SiO_2 > 70 wt%) cannot form by extreme fractionation of mafic magmas with low water contents because the optimal crystallinity window for physical separation of crystals and liquids has a theoretical range of 50–70 vol% (e.g., Dufek and Bachmann, 2010). Alternatively, the Huidong granites may form by partial melting of juvenile mafic crust. If this is the case, the degree of melting could be very low, close to 10% based on our equilibrium modelling. Nevertheless, it is not yet fully understood whether melts produced from such small degrees of melting may be extracted from the source region.

Although it is difficult to distinguish fractional crystallization and partial melting models for the Huidong granites based on geochemical modelling, we identify that the Huidong granites show features of extensive fractional crystallization. The depletion in MgO, CaO and Al_2O_3, and enrichment in $Fe_2O_3{}^T$ of the Huidong granites may be resulted from fractionation of Mg-Ca-Al rich minerals, such as spinel, pyroxenes and alkali feldspars. Fractionation of these minerals can also explain the strong negative anomalies of Ba, Sr and Ti in primitive mantle normalized trace element distribution patterns, which are identical to the highly-evolved mantle-derived Cida A-type granites in ELIP (Fig. 6). Besides, the Huidong rocks represent some of the hottest granites in the world according to zircon saturation temperature (1031–1139 °C, average 1081 °C; Table 3) estimated using the equation proposed by Boehnke et al. (2013). From this view, we prefer fractional crystallization of tholeiitic magmas model for the generation of the small-scale Huidong pluton, even though melting of hot juvenile crust model could not be ruled out.

The Huidong granites have zircon oxygen isotopes ~1–2‰ higher than the 'mantle zircon' value (Fig. 8). We suggest that this is not a result of fractionation because zircons from similarly evolved plagiogranite have zircon oxygen isotope similar to 5.3‰ (Grimes et al., 2013). High-$\delta^{18}O$ materials may have been introduced to the source region prior to mantle melting. Alternatively, they may be involved in the evolution of the Huidong parental magmas through crustal assimilation.

5.2.2. Formation of Yuanmou A-type granites by ancient crustal melting

As shown above, the Yuanmou granites show geochemical and features remarkably different from the Huidong granites (Figs. 4, 6, 7 and 9). In particular, they have less radiogenic Nd-Hf isotopes (Fig. 7). They also have much higher Th/Nb ratios similar to other 1.02–1.05 Ga felsic rocks in the region (Fig. 10). We suggest that the Yuanmou granites could have formed by melting of pre-existing crustal rocks. As is demonstrated in Fig. 7, the Yuanmou granites have Nd-Hf isotopes plotting close to the crustal evolution path of those of the ~1.7 Ga mafic rocks, but tending towards those of the Huidong granites. Zircon $\varepsilon_{Hf}(t)$ of the Yuanmou granites vary from −1.5 to +5.1, suggesting that there may be some contributions from mantle-derived material in the genesis of the Yuanmou granites.

5.3. Geological implications

Globally, A-type granites are typically associated with belt of anorogenic igneous rocks (Loiselle and Wones, 1979; Whalen et al., 1987). Using trace element discrimination diagrams, both Huidong and Yuanmou granites are plotted in the within-plate granite (WPG) field (Fig. 12). Previous studies on ~1.02–1.05 Ga felsic rocks also give the same results (e.g., Zhu et al., 2016; Chen et al., 2018). Along with the presence of coeval tholeiitic basalts and mafic dykes, geochemistry of the granites suggests an extensional setting for the bimodal magmatism, consistent with previous conclusions (e.g., Zhu et al., 2016; Chen et al.,

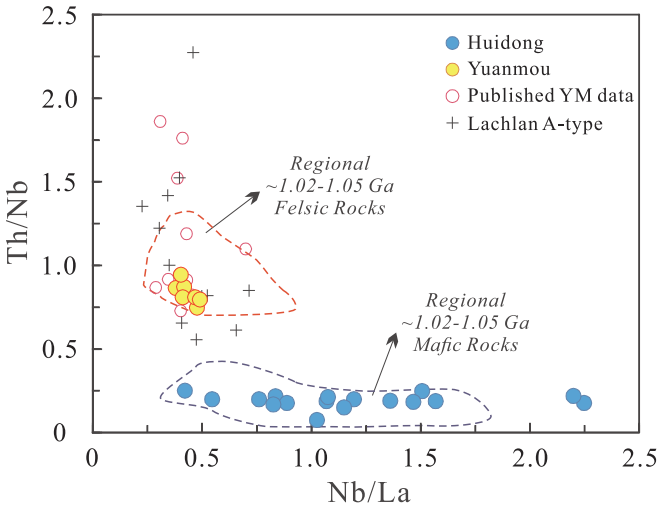

Fig. 10. Th/Nb vs. Nb/La diagram showing the Huidong granites have distinct Th-La-Nb characteristics with Yuanmou granites. Also shown are the plots of the ~ 1.02–1.05 Ga igneous rocks in the region (Greentree et al., 2006; Chen et al., 2014, 2018; Zhu et al., 2016) and Lachlan A-type rocks (Collins et al., under review).

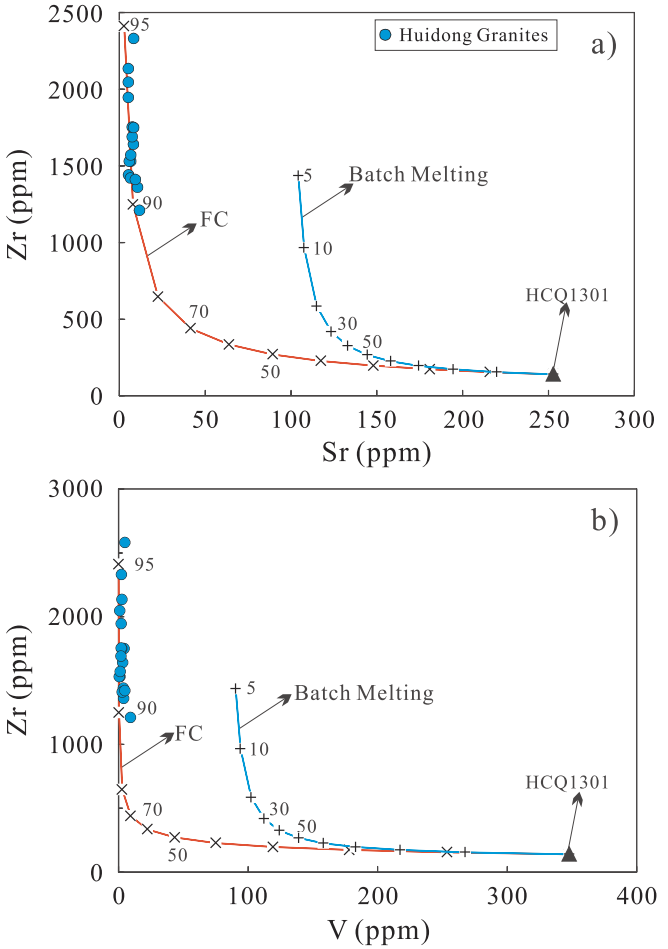

Fig. 11. Variation diagrams with batch melting and fractional crystallization (FC) models of compatible vs. incompatible trace elements for the Huidong granites. Partition coefficients are similar to those of Peccerillo et al. (2003). A mafic sample (HCQ1301; Rb 14.5 ppm, Sr 253 ppm, Ba 84.9 ppm, Zr 140 ppm, V 348 ppm) from the Huili dolerites (Zhu et al., 2016), which have similar Nd-Hf isotopic features with the Huidong granites, was used as the starting material for the modeling.

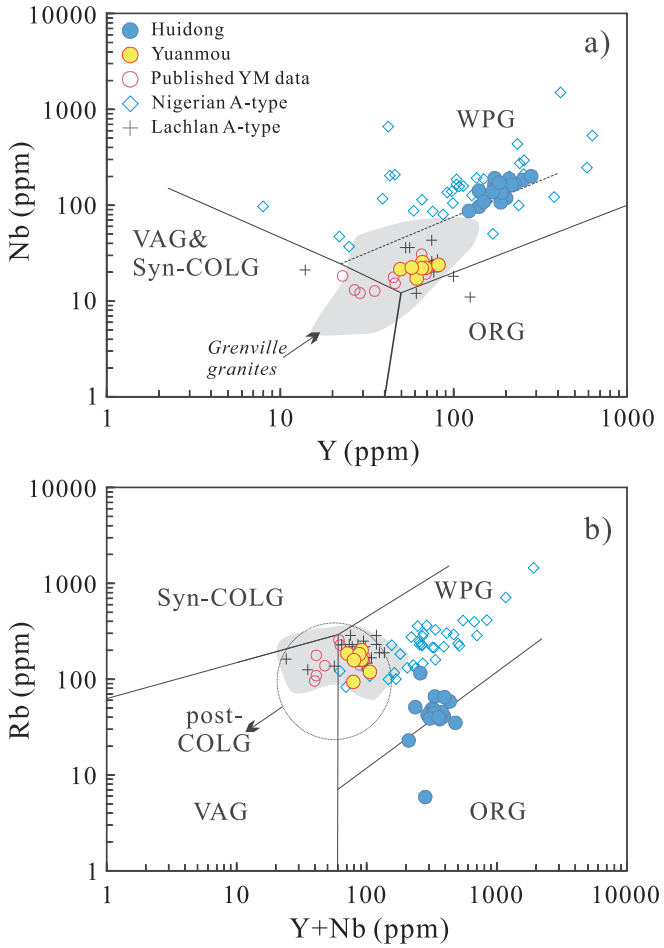

Fig. 12. (a) Nb versus Y and (b) Rb vs. Y + Nb diagrams of Pearce (1996) showing that the Huidong and Yuanmou granites rocks are mainly plotted into the field of within-plate granites (WPG). Abbreviations: VAG, volcanic arc granites; *syn*-COLG, *syn*-collisional granites; WPG, within-plate granites; ORG, ocean ridge granites. Also shown is the plots of the Lachlan and Nigerian A-type granites and Grenville granitoids.

2018).

We have compared our new data with published data of coeval granites in the region and A-type granitoids globally. We show that the Huidong granites have quite a few features similar to the Nigeria Younger granites, e.g., low CaO and Al_2O_3 and high HFSE (Fig. 4), consistent with their formation under high temperature (this study; Collins et al., 2018). However, the Huidong granites are more enriched in total iron and depleted in Rb, similar to ocean ridge granite (ORG in Fig. 12b). Furthermore, all ~1.04 Ga A-type granites in the western Yangtze are aluminous-peraluminous, distinct from the peralkaline granites that dominate the Nigeria Younger granite suite (Fig. 5), which is interpreted to have formed in a passive continental margin (Badejoko, 1986). By contrast, most of the ~1.04 Ga Yuanmou granites have compositions similar to A-types in the Paleozoic Lachlan Fold Belt in southeast Australia and late Mesoproterozoic granitoids (AMCG: anorthosite-mangerite-charnockite-granite) in the Grenville province (Figs. 4, 5, 9, 10 and 12). We suggest that formation of anorogenic igneous rocks does not necessarily argue against the presence of an orogenic belt.

In fact, anorogenic magmatism should form an integral part of the tectonic evolution of orogenic belts. In the Grenville Province of North America, at least three orogenic cycles can be recognized (McLelland and Daly, 1996; McLelland et al., 2010; Rivers, 1997, 2008). Anorogenic magmatism developed between 1.16 and 1.01 Ga (e.g, McLelland et al., 2004, 2010), typically at the waning stage of the orogeny

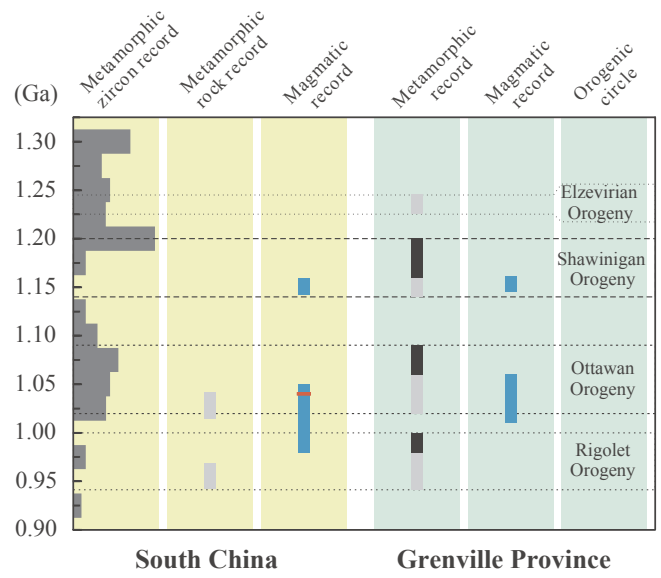

Fig. 13. 1.3–0.9 Ga metamorphic and magmatic record comparison between South China and Grenville province of North America. Black bars of metamorphic record are high-grade metamorphism; shallow grey bars are low-grade metamorphism. Deep grey specially denotes metamorphic zircon record in South China. Age data of Grenville Province come from McLelland et al. (1996, 2001, 2004, 2010) and Rivers (1997, 2008). Metamorphic data of South China are from Li et al. (2002, 2007) and Yao et al. (2017); magmatic records are compiled from Greentree et al. (2006), Li et al. (2013a), Chen et al. (2014, 2018), Zhu et al. (2016), Geng et al. (2017) and Wang et al. (2018).

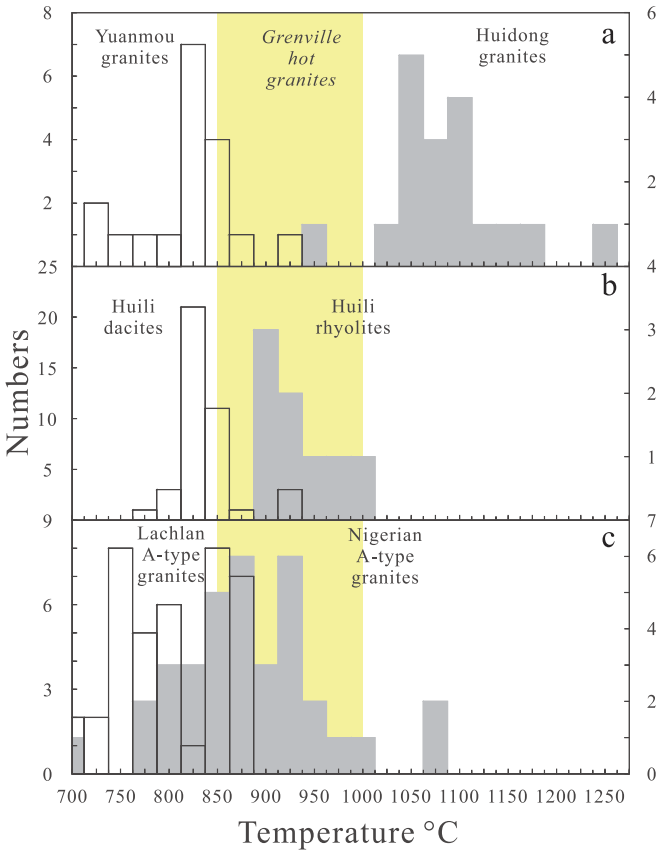

Fig. 14. Zircon saturation temperatures (after Boehnke et al. (2013)) for the 1.05–1.02 Ga felsic rocks in western Yangtze Block. Yellow area is plot of some hot Grenville granites with high temperature of 850–1000 °C (Moecher et al., 2014). Some T_{Zr} data of the Yuanmou granites are compiled from Chen et al. (2018). Left coordinate axis is for hollow bars; right coordinate axis is for grey bars. (For interpretation of the references to color in this figure legend, the reader is referred to the web version of this article.)

(McLelland et al., 2010). In Fig. 13, we demonstrate that the Yangtze Block may have experienced tectonic evolution history similar to that in the Grenville province during the late Mesoproterozoic time. Available geochronological data reveal two major Grenville-aged magmatic phases at 1159–1142 Ma and 1050–980 Ma. The former is represented by the ~1142 ± 16 Ma Laowushan alkali basalts (Greentree et al., 2006) in the western Yangtze Block and ~1159 ± 8 Ma Tieshajie A-type felsic volcanic rocks (Li et al., 2013a) in the eastern Yangtze Block. The latter magmatism is marked by the ~1050 Ma Julin tholeiitic basalts (Chen et al., 2014), the ~1050 Ma Huili rhyolites (Chen et al., 2018), the ~1043–1049 Ma Huidong granites (this study), the ~1041 Ma Yuanmou granites (Chen et al., 2018; this study), and the ~1025–1021 Ma Huili dacites and coeval Huili tholeiitic dolerites (Zhu et al., 2016; Geng et al., 2017) in the western Yangtze Block and the 1012–980 Ma Tieshajie OIB-like basalts (Wang et al., 2018) in the eastern Yangtze Block. The two magmatic events correspond to magmatism at 1160–1140 Ma and 1060–1010 Ma in the Grenville province (Rivers, 1997; McLelland and Daly, 1996; McLelland et al., 2001, 2010). On the other hand, metamorphic records as revealed by zircons with low Th/U (< 0.1) show that the Yangtze and Cathaysia Blocks may have experienced orogenic events at 1.21–1.17 Ga and 1.08–1.04 Ga (Fig. 13). Combined with the 1042–1015 Ma and 968–942 Ma metamorphism recorded by the Tianli Schists (Li et al., 2007), the Sibao Orogen could have undergone at least three cycles of orogeny, corresponding with the Shawinigan orogeny at 1200–1140 Ma, Ottawan orogeny at 1090–1020 Ma and Rigolet orogeny at 1000–940 Ma in the Grenville province (Rivers, 2008; McLelland et al., 2010). The temporal correlation in both metamorphic and magmatic records leads us to reinstate that the western Yangtze may form part of the Grenville orogen (Li et al., 2002).

As is demonstrated in Fig. 14, A-type granites in western Yangtze represent some of the hottest granites in the world, similar to hot Grenville granitoids in North America (Miller et al., 2003; Moecher et al., 2014). It appears that intrusion of mantle-derived magmas may have played an important role in their genesis. McLelland et al. (2010) proposed that the anorogenic magmatism in the Grenville province may have formed in an extensional setting due to repeated delamination of thickened lithosphere. Until highly potassic and high Sr/Y igneous records are found, we cannot verify the applicability of the model in South China.

As an alternative, we suggest that the orogenic cycles could have resulted from 'tectonic switching', similar to that proposed for the evolution of Tasmanides in eastern Australia (Collins, 2002; Kemp et al., 2009). The model is consistent with the formation of ~0.92–0.89 Ga arc magmatism (e.g., Ye et al., 2007; Li et al., 2009a), suggesting that subduction between Yangtze (eastern proto-Australia?) and Cathaysia (western Laurentia?) should have continued to that time. In western Yangtze, formation of MORB-like tholeiitic magmas and Huidong granites at ~1.04 Ga suggests that the lithosphere must have been greatly thinned at that time, likely due to formation of a nascent back arc, similar to that proposed for the formation of ~383–386 Ma dolerite dykes and A-type felsic rocks in the southern New England orogen (Offler and Huang, 2018). In the western Yangtze, no typical I- or S-type granites have been discovered yet. Interestingly, although I- and S-type granites are widely distributed in the Lachlan Fold belt to the south, very few have been found in the southern New England orogen, likely due to reworking of the orogen in late Paleozoic and Mesozoic time.

6. Conclusion

Huidong and Yuanmou granites in the western Yangtze were

emplaced at 1041–1049 Ma. The former has elemental and radiogenic Nd-Hf isotopic compositions that support its formation by extreme fractionation from mafic magmas, although partial melting of hot juvenile mafic crust could also be an alternative. By contrast, geochemistry of the Yuanmou granites suggests that it may form dominantly by melting pre-existing ancient crustal rocks. Despite difference in petrogenesis, both of them can be classified as aluminous A-type granites. Along with coeval tholeiitic magmatism, the anorogenic magmatism indicates an extensional environment in the late Mesoproterozoic.

Temporal correlation with metamorphic and magmatic records in the Grenville province suggests that the ~1.04 Ga A-type granites in the Yangtze Block may form part of the hot Grenville granitoid province. We suggest that their formation in the western Yangtze could be associated with development of a back-arc basin, resulted from retreat of a subduction system.

Acknowledgements

This study is supported by the National Natural Science Foundation of China (Grants 41572074 and 41273049). We thank Y. Liu, G.Q. Tang, Q.L. Li, and H. Tao for their assistance in SIMS dating. Mrs J. Hu, Y. Huang, and G.P. Bao are appreciated for their help in trace element analyses. Dr. C.F. Li is thanked for his effort in Nd isotopic analyses.

Appendix A. Supplementary data

Supplementary data to this article can be found online at https://doi.org/10.1016/j.precamres.2019.04.024.

References

Badejoko, T.A., 1986. The petrogenesis of the Younger Granites of Nigeria. J. Afr. Earth Sci. 5, 233–242.
Blichert-Toft, J., Albarede, F., 1997. The Lu-Hf geochemistry of chondrites and the evolution of the mantle–crust system. Earth Planet. Sci. Lett. 148, 243–258.
Boehnke, P., Watson, E.B., Trail, D., Harrison, T.M., Schmitt, A.K., 2013. Zircon saturation re-revisited. Chem. Geol. 351, 324–334.
Boynton, W.V., 1984. Geochemistry of the rare earth elements: meteorite studies. In: Henderson, P. (Ed.), Rare Earth Element Geochemistry. Elsevier, pp. 63–114.
Chen, W.T., Sun, W.H., Wang, W., Zhao, J.H., Zhou, M.F., 2014. "Grenvillian" intra-plate mafic magmatism in the southwestern Yangtze Block SW China. Precambrian Res. 242, 138–153.
Chen, W.T., Sun, W.H., Zhou, M.F., Wang, W., 2018. Ca. 1050 Ma intra-continental rift-related A-type felsic rocks in the southwestern Yangtze Block, South China. Precambrian Res. 309, 22–44.
Chen, W.T., Zhou, M.F., Zhao, X.F., 2013. Late Paleoproterozoic sedimentary and mafic rocks in the Hekou area, SW China: implication for the reconstruction of the Yangtze Block in Columbia. Precambrian Res. 231, 61–77.
Collins, W.J., 2002. Hot orogens, tectonic switching and creation of continental crust. Geology 30, 535–538.
Collins, W.J., Beams, S.D., White, A.J.R., Chappell, B.W., 1982. Nature and origin of A-type granites with particular reference to southeast Australia. Contrib. Mineral. Petrol. 80, 189–200.
Collins, W.J., Huang, H.Q., Bowden, P., 2018. Repeated S-I-A-type Granite Trilogy in the Lachlan Orogen, and Geochemical Contrasts with A-type Granites in Nigeria: Implications for Petrogenesis and Tectonic Discrimination. (Under review).
Cox, K.G., Bell, J.D., Pankhurst, R.J., 1979. In: The Interpretation of Igneous Rocks. Allen and Unwin, London, UK, pp. 450.
Dufek, J., Bachmann, O., 2010. Quantum magmatism: magmatic compositional gaps generated by melt-crystal dynamics. Geology 38, 687–690.
Eby, G.N., 1990. The A-type granitoids: a review of their occurrence and chemical characteristics and speculations on their petrogenesis. Lithos 26, 115–134.
Fan, H.P., Zhu, W.G., Li, Z.X., Zhong, H., Bai, Z.J., He, D.F., Chen, C.J., Cao, C.Y., 2013. Ca. 1.5 Ga mafic magmatism in South China during the break-up of the supercontinent Nuna/Columbia: the Zhuqing Fe-Ti-V oxide ore-bearing mafic intrusions in western Yangtze Block. Lithos 168–169, 85–98.
Fisher, C.F., Vervoort, J.D., Hanchar, J.M., 2014. Guidelines for reporting zircon Hf isotopic data by LA-MC-ICPMS and potential pitfalls in the interpretation of these data. Chem. Geol. 363, 125–133.
Frost, C.D., Frost, B.R., 1997. Reduced rapakivi-type granites: the tholeiite connection. Geology 25, 647–650.
Frost, C.D., Frost, B.R., 2011. On ferroan (A-type) granitoids: their compositional variability and modes of origin. J. Petrol. 52, 39–53.
Frost, C.D., Bell, J.M., Frost, B.R., Chamberiain, K.R., 2001. Crustal growth by magmatic underplating: isotopic evidence from the northern Sherman batholith. Geology 29, 515–518.
Gao, S., Yang, J., Zhou, L., Li, M., Hu, Z., Guo, J., Yuan, H., Gong, H., Xiao, G., Wei, J., 2011. Age and growth of the Archean Kongling terrain, South China, with emphasis on 3.3 Ga granitoid gneisses. Am. J. Sci. 311, 153–182.
Geng, Y.S., Kuang, H.W., Liu, Y.Q., Du, L.L., 2017. Subdivision and correlation of the Mesoproterozoic stratigraphy in the western and northern margins of Yangtze block. Acta Geol. Sin. 91, 2151–2174 (in Chinese with English abstract).
Geng, Y.S., Liu, Y.Q., Gao, L.Z., Peng, N., Jiang, X.J., 2012. Geochronology of the Mesoproterozoic Tong'an Formation in Southwestern margin of the Yangtze Craton: new evidence from zircon LA-ICP-MS U-Pb ages. Acta Geol. Sin. 86, 1479–1490 (in Chinese with English abstract).
Geng, Y.S., Yang, C.H., Du, L.L., Wang, X.S., Ren, L.D., Zhou, X.W., 2007. Chronology and tectonic environment of the Tianbaoshan Formation: new evidence from zircon SHRIMP U-Pb age and geochemistry. Geol. Rev. 53, 556–563 (in Chinese with English abstract).
Gorring, M.L., Estelle, T.C., Volkert, R.A., 2004. Geochemistry of the Late Mesoproterozoic Mount Eve Granite Suite: Implications for Late to post-Ottawan Tectonics in the New Jersey-Hudson Highlands. Geological Society of America Memoir No. 197, pp. 505–523.
Greentree, M.R., Li, Z.X., 2008. The oldest known rocks in south-western China: SHRIMP U-Pb magmatic crystallization age and detrital provenance analysis of the Paleoproterozoic Dahongshan Group. J. Asian Earth Sci. 33, 289–302.
Greentree, M.R., Li, Z.X., Li, X.H., Wu, H., 2006. Latest Mesoproterozoic to earliest Neoproterozoic basin record of the Sibao orogenesis in western South China and relationship to the assembly of Rodinia. Precambrian Res. 151, 79–100.
Griffin, W.L., Wang, X., Jackson, S.E., Pearson, N.J., O'Reilly, S.Y., Xu, X., Zhou, X., 2002. Zircon chemistry and magma mixing, SE China: in-situ analysis of Hf isotopes, Tonglu and Pingtan igneous complexes. Lithos 61, 237–269.
Grimes, C.B., Ushikubo, T., Kozdon, R., Valley, J.W., 2013. Perspectives on the origin of plagiogranite in ophiolites from oxygen isotopes in zircon. Lithos 179, 48–66.
Han, B.F., Wang, S.G., Jahn, B.M., Hong, D.W., Kagami, H., Sun, Y.L., 1997. Depleted-mantle source for the Ulungur River A-type granites from North Xinjiang, China: geochemistry and Nd–Sr isotopic evidence, and implications for Phanerozoic crustal growth. Chem. Geol. 138, 135–159.
Higgins, M.D., Breemen, O.V., 1996. Three generations of anorthosite-mangerite-charnockite-granite (AMCG) magmatism, contact metamorphism and tectonism in the Saguenay-Lac-Saint-Jean region of the Grenville Province, Canada. Precambrian Res. 79, 327–346.
Hu, Z.C., Liu, Y.S., Gao, S., Liu, W., Zhang, W., Tong, X., Lin, L., Zong, K., Li, M., Chen, H., Zhou, L., Yang, L., 2012. Improved in situ Hf isotope ratio analysis of zircon using newly designed X skimmer cone and jet sample cone in combination with the addition of nitrogen by laser ablation multiple collector ICP-MS. J. Anal. At. Spectrom. 27, 1391–1399.
Huang, H.Q., Li, X.H., Li, W.X., Li, Z.X., 2011. Formation of high $\delta^{18}O$ fayalite-bearing A-type granite by high-temperature melting of granulitic metasedimentary rocks, southern China. Geology 39, 903–906.
Hughes, S.S., Lewis, S.E., Bartholomew, M.J., Sinha, A.K., Herz, N., 2004. Geology and geochemistry of granitic and charnockitic rocks in the central Lovingston massif of the Grenvillian Blue Ridge terrane. In: Tollo, R.P., Corriveau, L., McLelland, J., Bartholomew, M.J. (Eds.), Proterozoic evolution of the Grenville orogen in North America. Geological Society of American Memoir No. 197, pp. 549–569.
Jeon, H., Williams, I.S., Chappell, B.W., 2012. Magma to mud to magma: Rapid crustal recycling by Permian granite magmatism near the eastern Gondwana margin. Earth Planet. Sci. Lett. 319–320, 104–117.
Jiao, S.J., Li, X.H., Huang, H.Q., Deng, X.G., 2015. Metasedimentary melting in the formation of charnockite: Petrological and zircon U-Pb-Hf-O isotope evidence from the Dahongshan S-type granitic complex in southern China. Lithos 239, 217–233.
Kemp, A.I.S., Hawkeworth, C.J., Collins, W.J., Gray, C.M., Blevin, P.L., EIMF, 2009. Isotopic evidence for rapid continental growth in an extensional accretionary orogen: the Tasmanides, eastern Australia. Earth Planet. Sci. Lett. 284, 455–466.
Kerr, A., Fryer, B.J., 1993. Nd isotope evidence for crust-mantle interaction in the generation of A-type granitoid suites in Labrador, Canada. Chem. Geol. 104, 39–60.
Lee, C.T., Bachmann, O., 2014. How important is the role of crystal fractionation in making intermediate magmas? Insights from Zr and P systematics. Earth Planet. Sci. Lett. 393, 266–274.
Li, L.M., Lin, S.F., Xing, G.F., Davis, D.W., Davis, W.J., Xiao, W.J., Yin, C.Q., 2013a. Geochemistry and tectonic implications of late Mesoproterozoic alkaline bimodal volcanic rocks from the Tieshajie Group in the southeastern Yangtze Block, South China. Precambrian Res. 230, 179–192.
Li, X.H., Li, W.X., Li, Z.X., Lo, C.H., Wang, J., Ye, M.F., Yang, Y.H., 2009a. Amalgamation between the Yangtze and Cathaysia Blocks in South China: Constraints from SHRIMP U-Pb zircon ages, geochemistry and Nd–Hf isotopes of the Shuangxiwu volcanic rocks. Precambrian Res. 174, 117–128.
Li, X.H., Liu, Y., Li, Q.L., Guo, C.H., Chamberlain, K.R., 2009b. Precise determination of Phanerozoic zircon Pb/Pb age by multi-collector SIMS without external standardization. Geochem. Geophys. Geosyst. 10, Q04010. https://doi.org/10.1029/2009GC002400.
Li, X.H., Tang, G.Q., Gong, B., Yang, Y.H., Hou, K.J., Hu, Z.C., Li, Q.L., Liu, Y., Li, W.X., 2013b. Qinghu zircon: a working reference for microbeam analysis of U-Pb age and Hf and O isotopes. Chin. Sci. Bull. 58, 4647–4654.
Li, Z.X., Bogdanova, S.V., Collins, A.S., Davidson, A., De Waele, B., Ernst, R.E., Fitzsimons, I.C.W., Fuck, R.A., Gladkochub, D.P., Jacobs, J., Karlstrom, K.E., Lu, S., Natapovm, L.M., Pease, V., Pisarevsky, S.A., Thrane, K., Vernikovsky, V., 2008. Assembly, configuration, and break-up history of Rodinia: a synthesis. Precambrian Res. 160, 179–210.
Li, Z.X., Li, X.H., Zhou, H., Kinny, P.D., 2002. Grenville-aged continental collision in South China: new SHRIMP U-Pb zircon results and implications for Rodinia

configuration. Geology 30, 163–166.
Li, Z.X., Wartho, J.A., Occhipinti, S., Zhang, C.L., Li, X.H., Wang, J., Bao, C., 2007. Early history of the eastern Sibao orogen (South China) during the assembly of Rodinia: new 40Ar/39Ar dating and U-Pb SHRIMP detrital zircon provenance constraints. Precambrian Res. 159, 74–94.
Li, Z.X., Zhang, L., Powell, C.M., 1995. South China in Rodinia: part of the missing link between Australia-East Antarctica and Laurentia? Geology 23, 407–410.
Liu, Y.S., Gao, S., Hu, Z.C., Gao, C.G., Zong, K.Q., Wang, D., 2010. Continental and oceanic crust recycling-induced melt-peridotite interactions in the Trans-North China Orogen: U-Pb dating, Hf isotopes and trace elements in zircons of mantle xenoliths. J. Petrol. 51, 537–571.
Loiselle, M.C., Wones, D.R., 1979. Characteristics and origin of anorogenic granites. Geol. Soc. Am. Bull. Abstr. Prog. 92, 468.
McLelland, J.M., Bickford, M.E., Hill, B.M., Clechenko, C.C., Valley, J.W., Hamilton, M.A., 2004. Direct dating of Adirondack massif anorthosite by U-Pb SHRIMP analysis of igneous zircon: implications for AMCG complexes. Geol. Soc. Am. Bull. 116, 1299–1317.
McLelland, J.M., Daly, S.J., 1996. The Grenville orogenic cycle (ca. 1350–1000 Ma): an Adirondack perspective. Tectonophysics 265, 1–28.
McLelland, J.M., Hamilton, M.A., Selleck, B., McLelland, J.M., Walker, D., Orrell, S., 2001. Zircon U-Pb geochronology of the Ottawan Orogeny, Adirondack Highlands, New York: regional and tectonic implications. Precambrian Res. 109, 39–72.
McLelland, J.M., Selleck, B.W., Hamilton, M.A., Bickford, M.E., 2010. Late- to post-tectonic setting of some major Proterozoic anorthosite-mangerite-charnockite-granite (AMCG) suites. Can. Mineral. 48, 1025–1046.
Miller, C.F., McDowell, S.M., Mapes, R.W., 2003. Hot and cold granites? Implications of zircon saturation temperatures and preservation of inheritance. Geology 31 (6), 529–532.
Moecher, D.P., McDowell, S.M., Samson, S.D., Miller, C.F., 2014. Ti-in-zircon thermometry and crystallization modeling support hot Grenville granite hypothesis. Geology 42 (3), 267–270.
Morisset, C.E., Scoates, J.S., Weis, D., Friedman, R.M., 2009. U-Pb and 40Ar/39Ar geochronology of the Saint-Urbain and Lac Allard (Havre-Saint-Pierre) anorthosites and their associated Fe–Ti oxide ores, Québec: evidence for emplacement and slow cooling during the collisional Ottawan orogeny in the Grenville Province. Precambrian Res. 174, 95–116.
Offler, R., Huang, H.Q., 2018. Middle-Late Devonian nascent back arc formation, southern New England Orogen, NSW, Australia. Gondwana Res. 63, 250–267.
Paton, C., Woodhead, J.D., Hellstrom, J.C., Hergt, J.M., Greig, A., Maas, R., 2010. Improved laser ablation U-Pb zircon geochronology through robust downhole fractionation correction. Geochem. Geophys. Geosyst. 11, Q0AA06. https://doi.org/10.1029/2009GC002618.
Pearce, J.A., 1996. Sources and settings of granitic rocks. Episodes 19, 120–125.
Peccerillo, A., Barberio, M.R., Yirgu, G., Ayalew, D., Barbieri, M., Wu, T.W., 2003. Relationships between mafic and peralkaline silicic magmatism in continental rift settings: a petrological, geochemical and isotopic study of the Gedemsa Volcano, central Ethiopian rift. J. Petrol. 44, 2003–2032.
Qi, L., Hu, J., Grégoire, D.C., 2000. Determination of trace elements in granites by inductively coupled plasma mass spectrometry. Talanta 51, 507–513.
Qiu, Y.M., Gao, S., McNaughton, N.J., Groves, D.I., Ling, W., 2000. First evidence of > 3.2 Ga continental crust in the Yangtze craton of South China and its implications for Archean crustal evolution and Phanerozoic tectonics. Geology 28 (1), 11–14.
Quinn, R.J., 2012. The Evolution of Grenville Basement in the Eastern Great Smoky Mountains: Constraints from U-Pb Zircon Geochronology, Whole Rock Sm-Nd, and feldspar Pb geochemistry. [M.S. thesis]. University of Kentucky, Lexington, pp. 115.
Rivers, T., 1997. Lithotectonic elements of the Grenville province. Precambrian Res. 86, 117–154.
Rivers, T., 2008. Assembly and preservation of lower, mid, and upper orogenic crust in the Grenville Province—Implications for the evolution of large hot long-duration orogens. Precambrian Res. 167, 237–259.
SBG (Sichuan Bureau of Geology), 1967. A Report of Regional Geological Survey in Huili Area of the People's Republic of China (the scale of 1:200000). (in Chinese).
Söderlund, U., Patchett, P.J., Vervoort, J.D., Isachsen, C.E., 2004. The Lu-176 decay constant determined by Lu-Hf and U-Pb isotope systematics of Precambrian mafic intrusions. Earth Planet. Sci. Lett. 219, 311–324.
Sun, S.S., McDonough, W.F., 1989. Chemical and isotopic systematics of oceanic basalts: implications for mantle composition and processes. In: Saunders, A.D., Norry, M.J. (Eds.), Magmatism in the Ocean Basins. Geological Society, London, pp. 313–345 Special Publications, no. 42.
Tollo, R.P., Aleinikoff, J.N., Borduas, E.A., Hackley, P.C., Fanning, C.M., 2004. Petrologic and geochronologic evolution of the Grenville orogeny, northern Blue Ridge Province, Viriginia. In: Tollo, R.P. (Ed.), Proterozoic Tectonic Evolution of the Grenville Orogen in North America. Geological Society of America Memoir No. 197, pp. 647–678.
Turner, S.P., Foden, J.D., Morrison, R.S., 1992. Derivation of A-type magmas by fractionation of basaltic magma: an example from the Padthaway Ridge, South Australia. Lithos 28, 151–179.
Valley, J.W., Lackey, J.S., Cavosie, A.J., Clechenko, C.C., Spicuzza, M.J., Basei, M.A.S., Bindeman, I.N., Ferreira, V.P., Sial, A.N., King, E.M., Peck, W.H., Sinha, A.K., Wei, C.S., 2005. 4.4 billion years of crustal maturation: oxygen isotope ratios of magmatic zircon. Contrib. Mineral. Petrol. 150, 561–580.
Wang, G.G., Ni, P., Zhu, A.D., Wang, X.L., Li, L., Hu, J.S., Lin, W.H., Huang, B., 2018. 1.01–0.98 Ga mafic intra-plate magmatism and related Cu-Au mineralization in the eastern Jiangnan orogen: evidence from Liujia and Tieshajie basalts. Precambrian Res. 309, 6–21.
Wang, L.J., Yu, J.H., Griffin, W.L., O'Reilly, S.Y., 2012a. Early crustal evolution in the western Yangtze Block: evidence from U-Pb and Lu-Hf isotopes on detrital zircons from sedimentary rocks. Precambrian Res. 222–223, 368–385.
Wang, W., Zhou, M.F., Yan, D.P., Li, L., John, M., 2013. Detrital zircon record of Neoproterozoic active-margin sedimentation in the eastern Jiangnan Orogen, South China. Precambrian Res. 235, 1–19.
Wang, X.L., Zhou, J.C., Griffin, W.L., Wang, R.C., Qiu, J.S., O'Reilly, S.Y., Xu, X.S., Liu, X.M., Zhang, G.L., 2007. Detrital zircon geochronology of Precambrian basement sequences in the Jiangnan orogen: dating the assembly of the Yangtze and Cathaysia blocks. Precambrian Res. 159, 117–131.
Whalen, J.B., Currie, K.L., Chappell, B.W., 1987. A-type granites: geochemical characteristics, discrimination and petrogenesis. Contrib. Mineral. Petrol. 95, 407–419.
Yang, C.H., Geng, Y.S., Du, L.L., Ren, L.D., Wang, X.S., Zhou, X.W., Yang, Z.S., 2009. The identification of the Grenvillian granite on the western margin of the Yangtze Block and its geological implications. Geol. China 36, 647–657 (in Chinese with English Abstract).
Yang, J.H., Wu, F.Y., Wilde, S.A., Xie, L.W., Yang, Y.H., Liu, X.M., 2007. Tracing magma mixing in granite genesis: in situ U-Pb dating and Hf-isotope analysis of zircons. Contrib. Mineral. Petrol. 153, 177–190.
Yao, W.H., Li, Z.X., Li, W.X., Li, X.H., 2017. Proterozoic tectonics of Hainan Island in supercontinent cycles: new insights from geochronological and isotopic results. Precambrian Res. 290, 86–100.
Ye, M.F., Li, X.H., Li, W.X., Liu, Y., Li, Z.X., 2007. SHRIMP zircon U-Pb geochronological and whole-rock geochemical evidence for an early Neoproterozoic Sibaoan magmatic arc along the southeastern margin of the Yangtze block. Gondwana Res. 12, 144–156.
Zhang, C.H., Gao, L.Z., Wu, Z.J., Shi, X.Y., Yan, Q.R., Li, D.J., 2007. SHRIMP U-Pb zircon age of tuff from the Kunyang Group in central Yunnan: Evidence for Grenvillian orogeny in South China. Chin. Sci. Bull. 52, 1517–1525.
Zhang, S.B., Zheng, Y.F., Wu, Y.B., Zhao, Z.F., Gao, S., Wu, F.Y., 2006. Zircon isotope evidence for ≥3.5 Ga continental crust in the Yangtze craton of China. Precambrian Res. 146, 16–34.
Zhao, J.H., Zhou, M.F., Yan, D.P., Zheng, J.P., Li, J.W., 2011. Reappraisal of the ages of Neoproterozoic strata in South China: no connection with the Grenvillian orogeny. Geology 39, 299–302.
Zhao, X.F., Zhou, M.F., Li, J.W., Sun, M., Gao, J.F., Sun, W.H., Yang, J.H., 2010. Late Paleoproterozoic to early Mesoproterozoic Dongchuan Group in Yunnan, SW China: Implications for tectonic evolution of the Yangtze Block. Precambrian Res. 182, 57–69.
Zheng, J.P., Griffin, W.L., O'Reilly, S.Y., Zhang, M., Pearson, N., Pan, Y., 2006. Widespread Archean basement beneath the Yangtze Craton. Geology 34, 417–420.
Zhong, H., Zhu, W.G., Chu, Z.Y., He, D.F., Song, X.Y., 2007. Shrimp U-Pb zircon geochronology, geochemistry, and Nd-Sr isotopic study of contrasting granites in the Emeishan large igneous province, SW China. Chem. Geol. 236, 112–133.
Zhu, W.G., Zhong, H., Li, Z.X., Bai, Z.J., Yang, Y.J., 2016. SIMS zircon U-Pb ages, geochemistry and Nd-Hf isotopes of ca. 1.0 Ga mafic dykes and volcanic rocks in the Huili area, SW China: origin and tectonic significance. Precambrian Res. 273, 67–89.
Zhu, W.G., Bai, Z.J., Zhong, H., Ye, X.T., Fan, H.P., 2017. The origin of the ca. 1.7 Ga gabbroic intrusion in the Hekou area, SW China: constraints from SIMS U-Pb zircon geochronology and elemental and Nd isotopic geochemistry. Geol. Mag. 154 (2), 286–304.